H H AEROSPACE DESIGN CO., INC.

DYNAMIC FRACTURE IN ORTHOTROPIC
FIBER COMPOSITES

James H. Williams, Jr.
Petros N. Kousiounelos
Samson S. Lee

Submitted to the
Naval Air Systems Command

First Annual Report
Contract No. N00019-77-C-0294

May 1978

78 14 08 180

SECURITY CLASSIFICATION OF THIS PAGE (When Data Entered)

REPORT DOCUMENTATION PAGE		READ INSTRUCTIONS BEFORE COMPLETING FORM
1. REPORT NUMBER	2. GOVT ACCESSION NO.	3. RECIPIENT'S CATALOG NUMBER
4. TITLE (and Subtitle) DYNAMIC FRACTURE IN ORTHOTROPIC FIBER COMPOSITES		5. TYPE OF REPORT & PERIOD COVERED FINAL REPORT APRIL 1977-APRIL 1978
		6. PERFORMING ORG. REPORT NUMBER
7. AUTHOR(s) James H. Williams, Jr. Petros N. Kousiounelos Samson S. Lee		8. CONTRACT OR GRANT NUMBER(s) N00019-77-C-0294
9. PERFORMING ORGANIZATION NAME AND ADDRESS H H Aerospace Design Co., Inc. 299 Broadway New York, NY 10007		10. PROGRAM ELEMENT, PROJECT, TASK AREA & WORK UNIT NUMBERS
11. CONTROLLING OFFICE NAME AND ADDRESS		12. REPORT DATE May 1978
		13. NUMBER OF PAGES
14. MONITORING AGENCY NAME & ADDRESS(if different from Controlling Office) Naval Air Systems Command Washington, D.C. 20361 Code: AIR-52032D		15. SECURITY CLASS. (of this report) UNCLASSIFIED
		15a. DECLASSIFICATION/DOWNGRADING SCHEDULE

16. DISTRIBUTION STATEMENT (of this Report)

Distribution Unlimited

APPROVED FOR PUBLIC RELEASE:
DISTRIBUTION UNLIMITED

17. DISTRIBUTION STATEMENT (of the abstract entered in Block 20, if different from Report)

Distribution Unlimited

103 p.

18. SUPPLEMENTARY NOTES

Annual rept. no. 1 (Final), Apr 77-Apr 78,

19. KEY WORDS (Continue on reverse side if necessary and identify by block number)

Dynamic Fracture
Composite Materials
Crack Arrest

20. ABSTRACT (Continue on reverse side if necessary and identify by block number)

The underlying principles of dynamic fracture and crack arrest in fiber composites are reviewed in terms of the conservation of mechanical energy. An approximate Mode I dynamic crack extension force for a highly orthotropic 0° unidirectional fiber composite is derived.

(continued)

0 DEGREE

DD FORM 1473 EDITION OF 1 NOV 65 IS OBSOLETE
1 JAN 73

410837

SECURITY CLASSIFICATION OF THIS PAGE (When Data Entered)

78 14 08 180

The governing partial differential equations for dynamic crack propagation in double cantilever beam unidirectional composite specimens are derived. A finite-difference scheme for solving these equations is presented along with the stability and convergence criteria for a numerical solution.
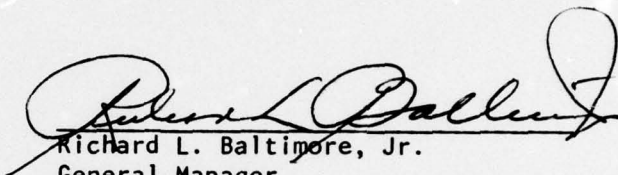
A conductive grid system for measuring the crack-tip velocity profile is described. This system is capable of assisting in the measurement of the dynamic fracture toughness of fiber composites.

FOREWORD

This report has been prepared as part of NAVAIR Contract No. N00019-77-C-0294 by Dr. James H. Williams, Jr. who is Chief Consultant and a Principal Consulting Investigator on the staff of H H Aerospace Design Co., Inc. in addition to serving as a tenured faculty member in the Department of Mechanical Engineering at the Massachusetts Institute of Technology.

Richard L. Baltimore, Jr.
General Manager
H H Aerospace Design Co., Inc.

iii

CONTENTS

CONTENTS (continued)

SECTION I

DYNAMIC FRACTURE AND CRACK ARREST

ABSTRACT

The underlying principles of dynamic fracture and crack arrest
in fiber composite materials are described in terms of the conservation
of mechanical energy.

INTRODUCTION

The fail-safe design philosophy requires that

(1) the damage in a structure can be detected before
    it reaches a critical size, and

(2) even if a critical flaw becomes unstable, the structure
    will have a mode of crack arrest that will provide
    enough residual strength and stiffness to allow time
    for corrective measures.

Because of the quasi-brittle mode of failure exhibited by graphite
fiber composites, the development of crack arrest concepts should be
an important part in any overall structures program involving these
materials.

The underlying principle of crack arrestment is to reduce the
crack extension (driving) force below the resisting force that must
be exceeded in order to extend the crack. This concept leads to a
set of general classifications of crack arresters, namely:

1. Arresters that decrease the crack driving force on a
   propagating crack. (For example, a skin-stringer system
   in which the stringer reduces the driving force on the
   crack in the skin.)

2. Arresters that increase the material fracture toughness
   encountered by the propagating crack. (For example,
   integral "toughening" or "softening" strips in a primary
   panel.)

3. Arresters that both decrease the crack driving force and
   increase the material toughness.

-3-

CRACK ARREST IN COMPOSITE STRUCTURES

There are two distinct basic crack arrest concepts as described in the Introduction. These two techniques are illustrated in Fig. 1. A primary laminate without arrest capability is shown in Fig. 1a. In Fig. 1b the crack is arrested by the second category by inserting an arrester laminate having a high dynamic fracture toughness. The first category is represented in Fig. 1c where the addition of a stiffener reduces the local crack driving force. In both Figs. 1b and 1c there is some return of the kinetic energy which must be "absorbed" by the arrester.

There are only a few papers in the open literature relating to crack arrestment in advanced fiber composite structures. The buffer strip (arrester laminate; Fig. 1b) concept has been shown to be capable of providing crack arrestment in graphite fiber epoxy laminates. Eisenmann and Kaminski [1]*, Bhatia and Verette [2], Sendeckyj [3], and Hess et al. [4] used the two-parameter description of fracture in composites proposed by Waddoups et al. [5] to predict the strength of panels containing an arrested crack.

All of the above crack arrest analyses for composites are based on static stress analysis. However, crack arrest, being a dynamic process, can be accurately modeled only by a dynamic fracture analysis. It has been shown [6] rather dramatically that statically-based crack arrest analyses can seriously overestimate a structure's crack arrest capability. This potentially dangerous statically-based overestimation

---

*Numbers in square brackets indicate references at the end of each section of the report.

-5-

is due to the facts that static calculations (1) cannot account for
the return of kinetic energy to the crack tip and (2) must assume that
the fracture energy is a constant that is independent of the crack pro-
pagation speeds. The first of these dynamic requirements is a function
of the geometry of the structure and is automatically included in any
fully dynamic fracture analysis. The second requirement is accommodated
via a dynamic fracture toughness which is a material property.

DYNAMIC FRACTURE AND CRACK ARREST ANALYSES

If a crack is extending, the conservation of mechanical energy
requires that

$$\frac{dW}{dA} = \frac{dU}{dA} + \frac{dT}{dA} + R \tag{1}$$

where W is the work done on the structure by the external forces, U is
the stored elastic strain energy, T is the kinetic energy, A is the
crack area, and R is the dynamic fracture toughness of the material.
The dynamic crack extension force $\mathcal{G}$ is defined by

$$\mathcal{G} = \frac{dW}{dA} - \frac{dU}{dA} - \frac{dT}{dA} . \tag{2}$$

Thus, from the principle of conservation of mechanical energy,
crack extension or continued propagation will occur when

$$\mathcal{G}(a,t) = R(\dot{a}) \tag{3}$$

and, no crack growth occurs or crack arrest results when

$$\mathcal{G}(a,t) < R(\dot{a}) \tag{4}$$

where a is the crack length, $\dot{a}$ is the crack-tip velocity and t is time.[*]
There is both theoretical and experimental evidence [7-12] that in homo-
geneous isotropic materials $\mathcal{G}$ is a function of crack length (a) and time
(t), and that R is a material property that is dependent primarily on

―――――――――――――――――――

[*]Note that the condition $\mathcal{G}(a,t) > R(\dot{a})$ would violate the principle of
conservation of mechanical energy and therefore, cannot exist.

the propagation velocity ($\dot{a}$); hence the functional dependencies indicated in eqns. (3) and (4). Whereas $R(\dot{a})$ has been determined for a number of homogeneous isotropic materials, it has not been determined for any of the fiber composites.

REFERENCES

1. Eisenmann, J.R. and Kaminski, B.E., "Fracture Control for Composite Structures", Engineering Fracture Mechanics, 1972, Vol. 4, pp. 907-913.

2. Bhatia, N.M. and Verette, R.M., "Crack Arrestment of Laminated Composites", Fracture Mechanics of Composites, ASTM STP 593. American Society for Testing and Materials, 1975, pp. 200-214.

3. Sendeckyj, G.P., "Concepts for Crack Arrestment in Composites", Fracture Mechanics of Composites, ASTM STP 593, American Society for Testing and Materials, 1975, pp. 215-226.

4. T.E. Hess, S.L. Huang and H. Rubin, "Fracture Control in Composite Materials Using Integral Crack Arresters", Journal of Aircraft, Vol. 14, No. 10, October 1977, pp. 994-999.

5. Waddoups, M.E., Eisenmann, J.R., and Kaminski, B.E., "Macroscopic Fracture Mechanisms of Advanced Composite Materials", J. Composite Materials, Vol. 5, October 1971, pp. 446-454.

6. M. Kanninen, E. Mills, G. Hahn, C. Marschall, D. Borek, A. Coyle, K. Masubuchi, and K. Itoga, "A Study of Ship Hull Crack Arrester Systems", Dept. of the Navy, NAVSHIPS No. 0988-071-6010, December 1975.

7. R.G. Hoagland, A.R. Rosenfield, and G.T. Hahn, "Mechanisms of Fast Fracture and Arrest in Steels", Metallurgical Transactions, Vol. 3, January 1972, pp. 123-136.

8. T.L. Paxson, and R.A. Lucas, "An Experimental Investigation of the Velocity Characteristics of a Fixed Boundary Model, Proc. on Dynamic Crack Propagation", Sih, ed., Noordhoff International Publishing, Leyden, July 1972, pp. 415-426.

9. G.T. Hahn, R.G. Hoagland, M.F. Kanninen, A.R. Rosenfield, and Sejnoha, R., "Fast Fracture Resistance and Crack Arrest in Structural Steels", Report SSC-252, Naval Ship Engineering Center, 1973.

10. H. Bergkvist, "The Motion of a Brittle Crack", Journal of the Mechanics and Physics of Solids, 1973, Vol. 21, pp. 229-239.

11. H. Bergkvist, "Crack Arrest in Elastic Sheets", Journal of the Mechanics and Physics of Solids, 1974, Vol. 22, pp. 491-502.

12. H. Bergkvist, "Some Experiments on Crack Motion and Arrest in Polymethylmethacrylate", Engineering Fracture Mechanics, 1974, Vol. 6, pp. 621-626.
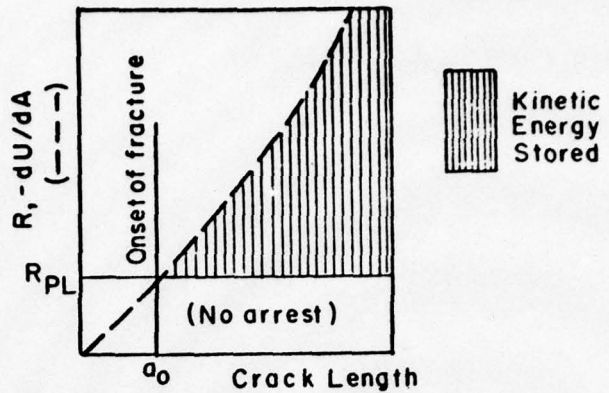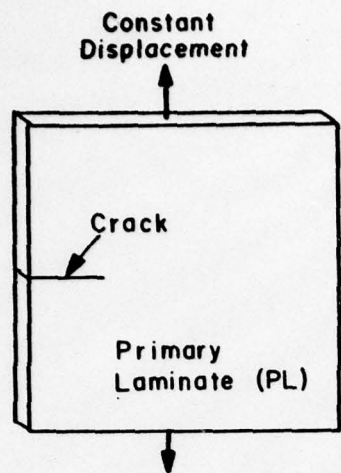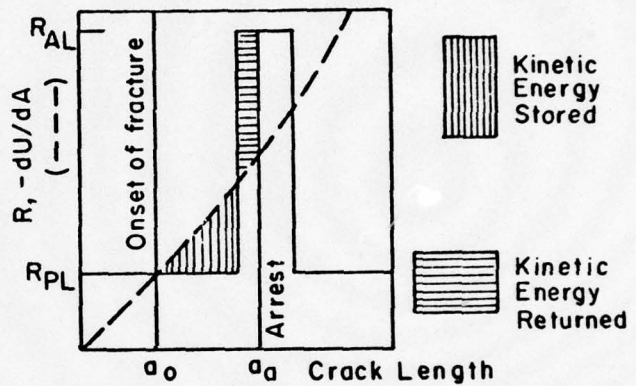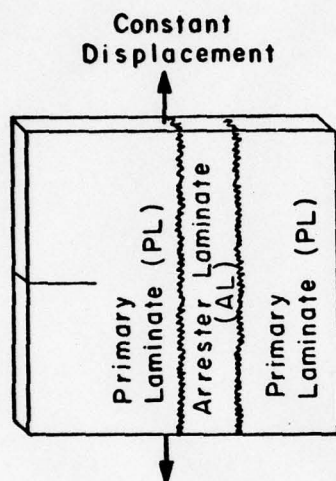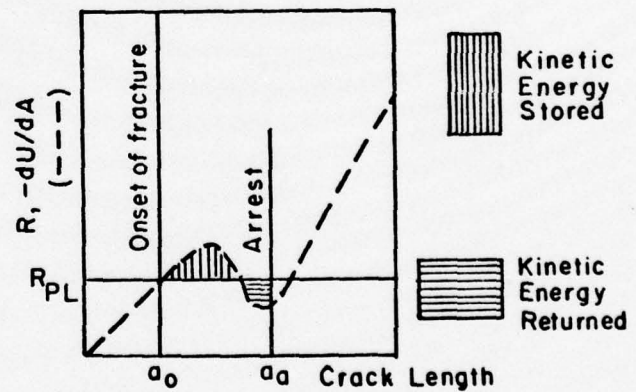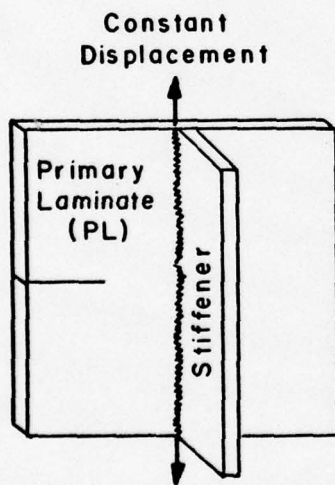
Fig. 1 Examples of Principal Concepts for Promoting Crack Arrest.
(a) Primary laminate cannot arrest an unstable crack;
(b) Primary laminate with arrester laminate which increases
the fracture toughness encountered by crack; and (c) Primary
laminate with stiffener which decreases the crack driving
force. (Also, see [6].)

-11-

SECTION 2

APPROXIMATE MODE I VELOCITY CORRECTION FACTOR FOR
0° UNIDIRECTIONAL FIBER COMPOSITES

ABSTRACT

An approximate Mode I dynamic crack extension force for a highly orthotropic 0° unidirectional fiber composite is derived in terms of the quasi-static crack extension force and a velocity correction factor. The analysis is based on the dynamic extension of a static Mode III isotropic/Mode I orthotropic analogy which was first recognized by F.A. McClintock. The complete dynamic analogies are given and the derived orthotropic velocity correction factor is compared with various isotropic velocity correction factors.

-13-

INTRODUCTION

The use of linear elastic fracture mechanics (LEFM) in the study of the onset of crack instability in brittle homogeneous isotropic materials is one of the modern accomplishments in mechanics. The onset of rapid fracture may be characterized by critical values of the static stress intensity factor k_s or the quasi-static crack extension force $\mathscr{G}_s^\dagger$ which have been shown [1] to be related, for example, as

$$\mathscr{G}_{s_{III}} = \frac{\left(k_{s_{III}}\right)^2}{2G} \qquad \text{for Mode III} \qquad (1)$$

where G is the shear modulus of the material. (Similar expressions can be written for Modes I and II.)

At present, it is generally accepted that for brittle homogeneous isotropic materials, the dynamic crack extension force $\mathscr{G}_d$ on a crack moving at constant velocity can be expressed as the product of $\mathscr{G}_s$ and a velocity correction factor $g(v)$ as [2,3]

$$\mathscr{G}_d = g(v)\, \mathscr{G}_s \qquad (2)$$

where $g(v)$ depends on the fracture mode and is a function of the material's dilatational, shear and Rayleigh wave speeds.

$\dagger$ $\mathscr{G}_s$ represents the nonrecoverable loss of energy per unit of crack extension and is also called the strain energy release rate. We prefer to call it the crack extension force or the crack driving force which we feel is particularly appropriate for dynamic analyses.

The purpose of this section is to present the derivation of an approximate velocity correction factor w(v) which is applicable to Mode I dynamic crack propagation in 0° unidirectional graphite fiber composites. The fiber composite is modeled as an equivalent homogeneous orthotropic material. The analysis is based on an extension of an analogy between the static Mode III crack-tip stress and displacement fields in homogeneous isotropic materials and the static Mode I crack-tip stress and displacement fields in homogeneous highly orthotropic materials. This analogy was first observed by McClintock [4]. Therefore, to the extent that it is useful to define a crack extension force or a critical stress intensity factor for fiber composite materials based upon such stress and displacement fields, the dynamic crack propagation in a fiber composite may be described in general terms by

$$\mathscr{G}_d^c = w(v)\,\mathscr{G}_s^c \tag{3}$$

where $\mathscr{G}_d^c$ and $\mathscr{G}_s^c$ are the dynamic and static composite crack extension forces, respectively.

-16-

THEORETICAL ANALYSIS

Analogy Between Mode III Isotropic and Mode I Orthotropic Static Crack-Tip Fields

In an unpublished paper, McClintock [4] described an analogy between the Mode III isotropic and the Mode I highly orthotropic crack-tip stress and displacement fields. Both the Mode III isotropic case and the Mode I highly orthotropic case are shown in Fig. 1. The Mode I highly orthotropic equations are approximate and are based on the assumption that $E_2 >> E_1$, where E_2 and E_1 are the extensional moduli orthogonal to and along the crack direction, respectively. This highly orthotropic require-ment is generally met by 0° unidirectional graphite fiber epoxy composites.

The static analogy provides functional equivalence between the following variables:

Mode III Isotropic		Mode I Orthotropic
$x_{1'}$	$\longrightarrow$	x_1
$x_{2'}$	$\longrightarrow$	$x_2 \sqrt{G_{12}/E_2}$
$u_{3'}$	$\longrightarrow$	u_2
G	$\longrightarrow$	$\sqrt{E_2 G_{12}}$ (4)
$\sigma_{1'3'}$	$\longrightarrow$	$\sigma_{12}\sqrt{E_2/G_{12}}$
$\sigma_{2'3'}$	$\longrightarrow$	σ_{22}
$k_{3'} = \sigma_{2'3'\infty}\sqrt{c'}$	$\longrightarrow$	$k_1 = \sigma_{22\infty}\sqrt{c}$

where the primed variables refer to Mode III isotropic and the unprimed variables refer to Mode I orthotropic. The x_i are the coordinates with the associated u_i displacements and the σ_{ij} stresses. G is the isotropic shear modulus and G_{12} is the in-plane orthotropic shear modulus. The static stress intensity factors are the k_i which are defined in terms of the stresses at infinity $\sigma_{ij\infty}$ and the crack lengths c' and c. A complete derivation of this analogy is given in the Appendix.

The extents to which the relevant equilibrium and constitutive equations are satisfied by the analogy will be examined next. These are

Mode III Isotropic	Mode I Orthotropic (Via Analogy)

Equilibrium: $\quad \dfrac{\partial \sigma_{1'3'}}{\partial x_{1'}} + \dfrac{\partial \sigma_{2'3'}}{\partial x_{2'}} = 0 \quad \longrightarrow \quad \dfrac{\partial \left(\sqrt{E_2/G_{12}}\ \sigma_{12} \right)}{\partial x_1} + \dfrac{\partial \sigma_{22}}{\partial \left(\sqrt{G_{12}/E_2}\ x_2 \right)} = 0$

or,

$$\frac{\partial \sigma_{12}}{\partial x_1} + \frac{\partial \sigma_{22}}{\partial x_2} = 0 \qquad (5)$$

Stress-Strain: $\quad \sigma_{1'3'} = G\,\dfrac{\partial u_{3'}}{\partial x_{1'}} \quad \longrightarrow \quad \sigma_{12}\sqrt{E_2/G_{12}} = \sqrt{E_2 G_{12}}\ \dfrac{\partial u_2}{\partial x_1}$

or,

$$\sigma_{12} = G_{12}\,\frac{\partial u_2}{\partial x_1} \qquad (6)$$

Stress-Strain: $\quad \sigma_{2'3'} = G\,\dfrac{\partial u_{3'}}{\partial x_{2'}} \quad \longrightarrow \quad \sigma_{22} = \sqrt{E_2 G_{12}}\ \dfrac{\partial u_2}{\partial \left(\sqrt{G_{12}/E_2}\ x_2 \right)}$

or,

$$\sigma_{22} = E_2\,\frac{\partial u_2}{\partial x_2} \qquad (7)$$

-18-

The equilibrium and constitutive equations for a 0° unidirectional composite as shown in Fig. 1(b) are [5]

Equilibrium: $\dfrac{\partial \sigma_{12}}{\partial x_1} + \dfrac{\partial \sigma_{22}}{\partial x_2} = 0$ (8)

Stress-Strain: $\sigma_{12} = G_{12}\left(\dfrac{\partial u_1}{\partial x_2} + \dfrac{\partial u_2}{\partial x_1}\right)$ (9)

and

$$\sigma_{22} - \nu_{21}\sigma_{11} = E_2 \dfrac{\partial u_2}{\partial x_2} . \tag{10}$$

It is clear that eqns. (5) and (8) are equivalent. However, the equivalences between eqns. (6) and (9) and between eqns. (7) and (10) are not so apparent. Eqns. (6) and (9) would be approximately equivalent if $\dfrac{\partial u_1}{\partial x_2}$ may be neglected when compared with $\dfrac{\partial u_2}{\partial x_1}$. In the Appendix this is shown to be consistent with other approximations which have already been made in deriving the analogy, eqns. (4). Also, eqns. (7) and (10) would be approximately equivalent if $\sigma_{22} \gg \nu_{21}\sigma_{11}$. This condition is shown to be satisfied also in the Appendix. Thus, the governing orthotropic field equations are consistent with the respective equations obtained via the analogy.

Extension of Analogy into the Dynamic Regime

In order to investigate the dynamic fracture of composites via the analogy, it is necessary to extend it into the dynamic regime. The additional analogous variables which must be obtained are the time and the

crack-tip velocity. (To date the crack-tip acceleration has not entered the solutions for the dynamic crack driving forces in isotropic materials, and thus the analogies developed here will not consider acceleration. However, we reserve judgment as to whether or not acceleration should be included in dynamic fracture analyses, and we shall consider this issue in a subsequent report.)

1. Analogy Between Times

The equations of motion for Mode III isotropic and Mode I ortho-tropic bodies are

Mode III Isotropic: $\qquad \dfrac{\partial \sigma_{1'3'}}{\partial x_{1'}} + \dfrac{\partial \sigma_{2'3'}}{\partial x_{2'}} = \rho' \dfrac{\partial^2 u_{3'}}{\partial t'^2}$ $\qquad\qquad$ (11)

Mode I Orthotropic: $\qquad \dfrac{\partial \sigma_{12}}{\partial x_1} + \dfrac{\partial \sigma_{22}}{\partial x_2} = \rho \dfrac{\partial^2 u_2}{\partial t^2}$ $\qquad\qquad$ (12)

where ρ' and ρ are the Mode III isotropic and Mode I orthotropic mass densities, respectively, and t' and t are the respective times. Assuming that there is an analogy between t' and t such that $t' \rightarrow \alpha t$, where α is a proportionality constant, α may be determined by substituting the analogy represented by eqns. (4) into eqn. (11) which gives

$$\frac{\partial \sigma_{22}}{\partial \left(\sqrt{G_{12}/E_2}\; x_2\right)} + \frac{\partial \left(\sqrt{E_2/G_{12}}\, \sigma_{12}\right)}{\partial x_1} = \rho \frac{\partial^2 u_2}{\partial (\alpha t)^2}$$

or,

$$\frac{\partial \sigma_{12}}{\partial x_1} + \frac{\partial \sigma_{22}}{\partial x_2} = \rho \sqrt{\frac{G_{12}}{E_2}}\; \frac{1}{\alpha^2}\; \frac{\partial^2 u_2}{\partial t^2} \quad . \qquad\qquad (13)$$

-20-

In order that eqns. (12) and (13) are equal, it is required that

$$\alpha = \left(\frac{G_{12}}{E_2}\right)^{1/4}.$$ (14)

Therefore, the analogy between times is

Mode III Isotropic   Mode I Orthotropic

$$t' \quad\longrightarrow\quad \left(\frac{G_{12}}{E_2}\right)^{1/4} t \ .$$ (15)

2. Analogy Between Velocities

Assuming a constant crack-tip velocity, the Mode III isotropic velocity V' may be found from

$$V' \cdot t' = \mathbf{X}_{1'} - c_o'$$ (16)

where $\mathbf{X}_{1'}$ is the horizontal axis ($x_{1'}$ direction) in a fixed reference frame and c_o' is the initial (or reference) crack length. Also, assuming that there is an analogy between the Mode III isotropic and the Mode I orthotropic velocities such that $V' \to \beta V$, where β is a proportionality constant and V is the Mode I orthotropic velocity, eqns. (4), (15) and (16) give

$$(\beta V)\left(\frac{G_{12}}{E_2}\right)^{1/4} t = \mathbf{X}_1 - c_o$$ (17)

-21-

where $\mathbf{X}_1$ is the Mode I orthotropic horizontal axis in a fixed reference frame and c_o is the initial (or reference) crack length. Furthermore, from kinematics

$$V \cdot t = \mathbf{X}_1 - c_o . \tag{18}$$

Combining eqns. (17) and (18) gives

$$\beta = \left(\frac{E_2}{G_{12}}\right)^{1/4} . \tag{19}$$

Therefore, the analogy between the crack propagation velocities is[†]

Mode III Isotropic	Mode I Orthotropic

$$V' \longrightarrow \left(\frac{E_2}{G_{12}}\right)^{1/4} V . \tag{20}$$

3. Analogy Between Crack Driving Forces

Kostrov and Nikitin [6] proved that for an elastic body in the absence of any thermal effects on the fracture process

$$\dot{\omega} = -v \lim_{\varepsilon \to o} \int_{x_{1B}}^{x_{1A}} (\sigma_{ij} \cdot u_{j,1}) \left|\begin{matrix} x_2 = +\varepsilon \\ \\ x_2 = -\varepsilon \end{matrix}\right. dx_1 \tag{21}$$

[†]Note that by considering the differential forms of eqns. (16) and (18), this derivation could have been performed for arbitrary crack velocities.

-22-

where $\dot{\omega}$ is the power of energy of fracture per unit length of crack, v is the crack-tip velocity, and $( )_{,1}$ denotes differentiation with respect to x_1. The integration contour for eqn. (21) is shown in Fig. 2. Eqn. (12) is valid for arbitrarily changing velocity as well as for constant velocity.

For the Mode III isotropic body, the only nonvanishing stress component that contributes to $\dot{\omega}$ is the shear stress $\sigma_{2'3'}$. Then, for this case, eqn. (21) can be written as

$$\dot{\omega}_{III(iso)} = -V' \lim_{\varepsilon' \to o} \int_{x_{1'B}}^{x_{1'A}} \left(\sigma_{2'3'} \frac{\partial u_{3'}}{\partial x_{1'}} \right) \Bigg|_{x_{2'} = -\varepsilon'}^{x_{2'} = +\varepsilon'} dx_{1'} \qquad (22)$$

where $\dot{\omega}_{III(iso)}$ is the Mode III isotropic power of energy of fracture per unit length of crack. Also, for the Mode I highly orthotropic body, the only nonvanishing stress component that contributes to $\dot{\omega}$ is the normal stress σ_{22}.[†] So,

$$\dot{\omega}_{I(ortho)} = -V \lim_{\varepsilon \to o} \int_{x_{1B}}^{x_{1A}} \left(\sigma_{22} \frac{\partial u_2}{\partial x_1} \right) \Bigg|_{x_2 = -\varepsilon}^{x_2 = +\varepsilon} dx_1 \qquad (23)$$

where $\dot{\omega}_{I(ortho)}$ is the Mode I orthotropic power of energy of fracture per unit length of crack.

[†] Due to elastic symmetry with respect to the x_1 axis, the shear stress σ_{12} along x_1 is zero and does not contribute to $\dot{\omega}$. See eqn. (A22) in the Appendix.

-23-

The relationship between $\dot{\omega}_j$ and the dynamic crack extension force $\mathcal{G}_{d:j}$ is given by [6]

$$\dot{\omega}_j = v \, \mathcal{G}_{d:j} \, . \tag{24}$$

So, from eqns. (22) and (24), the Mode III isotropic dynamic crack extension force $\mathcal{G}_{d:III(iso)}$ is

$$\mathcal{G}_{d:III(iso)} = -\lim_{\varepsilon' \to 0} \int_{x_1'B}^{x_1'A} \left(\sigma_{2'3'} \frac{\partial u_{3'}}{\partial x_{1'}} \right) \Bigg|_{x_2' = -\varepsilon'}^{x_2' = +\varepsilon'} dx_{1'} \, . \tag{25}$$

From eqns. (23) and (24), the Mode I orthotropic dynamic crack extension force $\mathcal{G}_{d:I(ortho)}$ is

$$\mathcal{G}_{d:I(ortho)} = -\lim_{\varepsilon \to 0} \int_{x_1B}^{x_1A} \left(\sigma_{22} \frac{\partial u_2}{\partial x_1} \right) \Bigg|_{x_2 = -\varepsilon}^{x_2 = +\varepsilon} dx_1 \, . \tag{26}$$

It is now necessary to establish the analogy between $\mathcal{G}_{d:III(iso)}$ and $\mathcal{G}_{d:I(ortho)}$. By using the analogy for $\sigma_{2'3'}$, $u_{3'}$, $x_{1'}$ and $x_{2'}$ which is given in eqns. (4), eqn. (25) gives

$$\mathcal{G}_{d:Anal} = -\lim_{\sqrt{\frac{G_{12}}{E_2}} \cdot \varepsilon \to 0} \int_{x_1B}^{x_1A} \left(\sigma_{22} \frac{\partial u_2}{\partial x_1} \right) \Bigg|_{x_2 = -\sqrt{\frac{G_{12}}{E_2}} \cdot \varepsilon}^{x_2 = +\sqrt{\frac{G_{12}}{E_2}} \cdot \varepsilon} dx_1 \tag{27}$$

-24-

where $\mathcal{G}_{d:Anal}$ represents the Mode III isotropic/Mode I orthotropic analogous dynamic crack extension force. Eqns. (26) and (27) differ only in the small quantities ε and $\sqrt{\dfrac{G_{12}}{E_2}} \cdot \varepsilon$ in the respective equations. However, because ε is arbitrary and tends to zero in the limit, eqns. (26) and (27) are equivalent and therefore $\mathcal{G}_{d:I(ortho)}$ is analogous to $\mathcal{G}_{d:III(iso)}$. Furthermore, because of the direct analogy[†] between the $\mathcal{G}_{d:j}$ as represented by eqns. (25) and (26), a direct analogy between the $\mathcal{G}_{s:j}$ follows because in the limit as $v \to 0$, eqns. (25) and (26) represent the expressions for the $\mathcal{G}_{s:j}$. Thus,

Mode III Isotropic   Mode I Orthotropic

$$\mathcal{G}_{s:III(iso)} \longrightarrow \mathcal{G}_{s:I(ortho)}$$

$$\text{(28)}$$

$$\mathcal{G}_{d:III(iso)} \longrightarrow \mathcal{G}_{d:I(ortho)}$$

[†]The phrase "direct analogy" is used to indicated that no multiplicative constants are required in order to complete the analogy. For example, the analogy between $x_{2'}$ and x_2 is not "direct" since the multiplicative constant $\sqrt{G_{12}/E_2}$ is required to complete it.

VELOCITY CORRECTION FACTOR

By using the analogies which have been presented, a velocity correction factor may be obtained. The velocity correction factor for the Mode III isotropic case is [8]

$$g_{III}(V') = \left[\frac{1 - \dfrac{V'}{c_s}}{1 + \dfrac{V'}{c_s}} \right]^{1/2} \tag{29}$$

where $c_s = (G/\rho')^{1/2}$ is the shear wave speed and ρ' is the mass density of the isotropic medium.

By assuming eqn. (2) to be a concept which is generic to dynamic fracture in any material, the following equations may be written:

$$\mathcal{G}_{d:III(iso)} = g_{III}(V') \; \mathcal{G}_{s:III(iso)}$$

$$\tag{30}$$

$$\mathcal{G}_{d:I(ortho)} = w_{I(0°)}(V) \; \mathcal{G}_{s:I(ortho)}$$

where the Mode I orthotropic velocity correction factor $w_{I(0°)}$ has been written with subscripts to denote its relationship to Mode I fracture in 0° unidirectional composites. Because of the direct analogies between the $\mathcal{G}_{s:j}$ and between the $\mathcal{G}_{d:j}$ as stated in eqns. (28), g_{III} and $w_{I(0°)}$ are directly analogous also. Thus, utilizing eqns. (4), (20) and (29) provides

-27-

$$w_{1(0°)}(V) = \left[\frac{1 - \dfrac{\left(E_2/G_{12}\right)^{1/4} V}{\left(\sqrt{G_{12}E_2}/\rho_c\right)^{1/2}}}{1 + \dfrac{\left(E_2/G_{12}\right)^{1/4} V}{\left(\sqrt{G_{12}E_2}/\rho_c\right)^{1/2}}} \right]^{1/2}$$

or,

$$w_{1(0°)}(V) = \left[\frac{1 - \dfrac{V}{C_s}}{1 + \dfrac{V}{C_s}} \right]^{1/2} \tag{31}$$

where $C_s = \left(G_{12}/\rho_c\right)^{1/2}$ is the composite shear wave speed and ρ_c is the composite mass density.

Eqn. (31) may be expressed in terms of the longitudinal wave speeds also. For example, along the stiffer modulus direction (x_2) the longitudinal wave speed is given by $C_2 = \left(E_2/\rho_c\right)^{1/2}$, and using this definition in C_s gives

$$C_s = \left(\frac{G_{12}}{E_2}\right)^{1/2} C_2 . \tag{32}$$

Substitution of eqn. (32) into eqn. (31) gives

$$w_{1(0°)}(V) = \left[\frac{1 - \left(\dfrac{E_2}{G_{12}}\right)^{1/2} \dfrac{V}{C_2}}{1 + \left(\dfrac{E_2}{G_{12}}\right)^{1/2} \dfrac{V}{C_2}} \right]^{1/2} . \tag{33}$$

-28-

Eqn. (31) is plotted in Fig. 3. For comparison, the Mode I
velocity correction factors for homogeneous isotropic elastic materials
as calculated by several researchers are shown also. The Broberg [9]
result which is for Poisson's ratio $\nu = \frac{2}{7}$ is for a crack which at time
t = 0 grows symmetrically from zero length at constant velocity. The
Freund [10] result which is for $\nu = \frac{1}{4}$ is for a semi-infinite crack
which at time t = 0 grows at constant velocity. The Rose [8] result is
simply a linear approximation of previous results. The most
striking feature of the $w_{I(0°)}$ computed here is that it does not go
to zero at ~$0.92 \frac{V}{C_s}$ which represents the Rayleigh wave speed for homo-
geneous isotropic materials. Also for V greater than zero, $w_{I(0°)}$ is
always greater than the isotropic velocity correction factors.

Eqn. (31) is plotted in Fig. 3. For comparison, the Mode I
velocity correction factors for homogeneous isotropic elastic materials
as calculated by several researchers are shown also. The Broberg [9]
result which is for Poisson's ratio $\nu = \frac{n}{4}$ is for a crack which at time
t = 0 grows symmetrically from zero length at constant velocity. The
Freund [10] result which is for $\nu = \frac{1}{4}$ is for a semi-infinite crack
which at time t = 0 grows at constant velocity. The Rose [8] result is
simply a linear approximation of previous results. The most
striking feature of the $w_I(v)$ computed here is that it does not go
to zero at $-0.92 \frac{v}{v_s}$ which represents the Rayleigh wave speed for homo-
geneous isotropic materials. Also for V greater than zero, $w_I(v)$ is
always greater than the isotropic velocity correction factors.

SUMMARY

The complete results for the Mode III isotropic/Mode I ortho-tropic dynamic crack propagation analogy are summarized in the Table below.

TABLE: Summary of Mode III Isotropic/Mode I Orthotropic Dynamic Fracture Analogy

Mode III Isotropic	Mode I Orthotropic
$x_{1'}$, (c')	x_1 , (c)
$x_{2'}$	$x_2 \sqrt{G_{12}/E_2}$
$u_{3'}$	u_2
G	$\sqrt{E_2 G_{12}}$
$\sigma_{1'3'}$	$\sigma_{12} \sqrt{E_2/G_{12}}$
$\sigma_{2'3'}$	σ_{22}
$k_{3'} = \sigma_{2'3'\infty} \sqrt{c'}$	$k_1 = \sigma_{22\infty} \sqrt{c}$
t'	$\left(G_{12}/E_2\right)^{1/4} t$
V'	$\left(E_2/G_{12}\right)^{1/4} V$
$\mathscr{G}_{s:III(iso)}$	$\mathscr{G}_{s:I(ortho)}$
$\mathscr{G}_{d:III(iso)}$	$\mathscr{G}_{d:I(ortho)}$
$g_{III}(V')$	$w_{I(0°)}(V)$

This analogy is valid under the assumptions that homogeneity and high orthotropy are adequately represented in the composite.

REFERENCES

1. J.L. Sanders, Jr., "On the Griffith-Irwin Fracture Theory", Trans. ASME, Series E, Journal of Applied Mechanics, Vol. 27, pp. 352-353, 1960.

2. E.H. Yoffé, "The Moving Griffith Crack", Phil. Mag., Vol. 42, pp. 739-750, 1951.

3. K.B. Broberg, "The Propagation of a Brittle Crack", Arkiv for Fysik, (18), pp. 159-192, 1960.

4. F.A. McClintock, "Problems in the Fracture of Composite Materials with Plastic Matrices", Dept. of Mech. Eng., M.I.T., March 1969, Unpublished Paper.

5. R.M. Jones, "Mechanics of Composite Materials", McGraw-Hill Book Co., Inc., 1975.

6. B.V. Kostrov and L.V. Nikitin, "Some General Problems of Mechanics of Brittle Fracture", Archiwum Mechaniki Stosowanej, 6, 22, pp. 749-776, 1970.

7. P.C. Paris and G.C. Sih, "Stress Analysis of Cracks", ASTM STP 381, American Society for Testing and Materials, pp. 30-83, 1965.

8. L.R.F. Rose, "Recent Theoretical and Experimental Results on Fast Brittle Fracture", International Jour. of Fracture, Vol. 12, No. 6, pp. 799-813, 1976.

9. K.B. Broberg, "Discussion of Fracture from the Energy Point of View", Recent Progress in Applied Mechanics, K.B. Broberg et. al. (eds.), Almqvist and Wicksell, Stockholm, pp. 125-151, 1967.

10. L.B. Freund, "Crack Propagation in an Elastic Solid Subjected to General Loading— I. Constant Rate of Extension", J. Mech. Phys. Solids, Vol. 20, pp. 129-140, 1972.
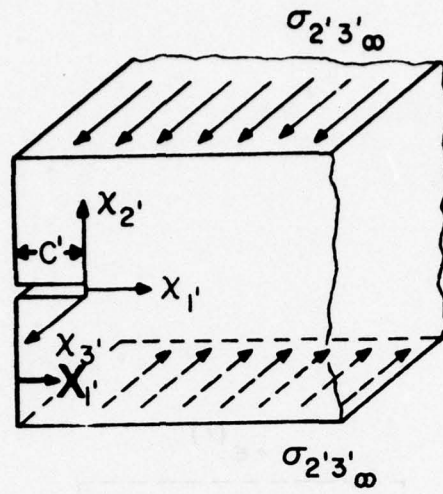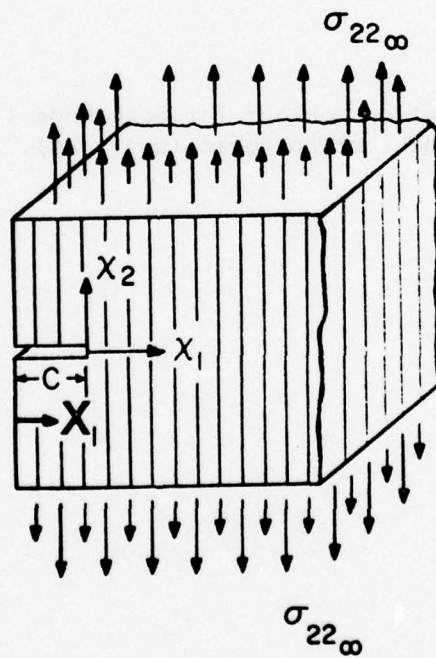
Fig. 1   a) Mode III isotropic case.
         b) Mode I 0° orthotropic case.
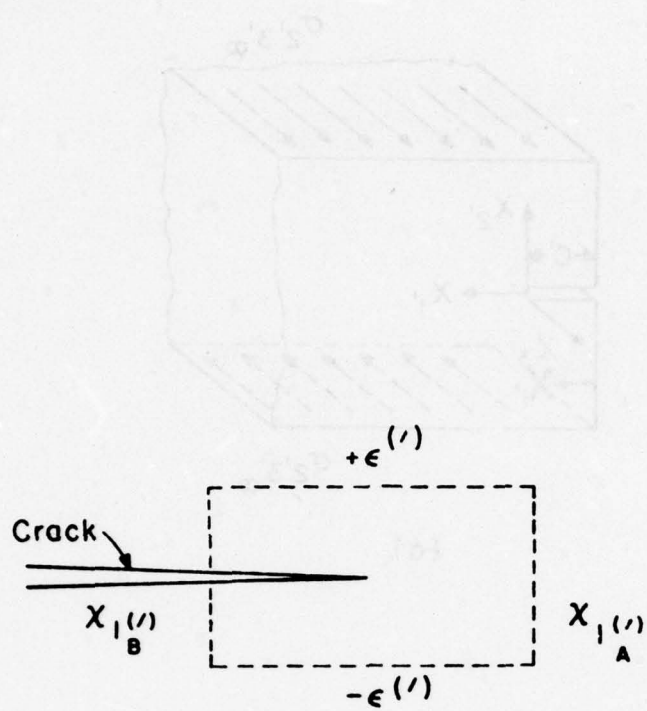
Fig. 2   Integration contour for both Mode III isotropic (')
and Mode I orthotropic (unprimed).
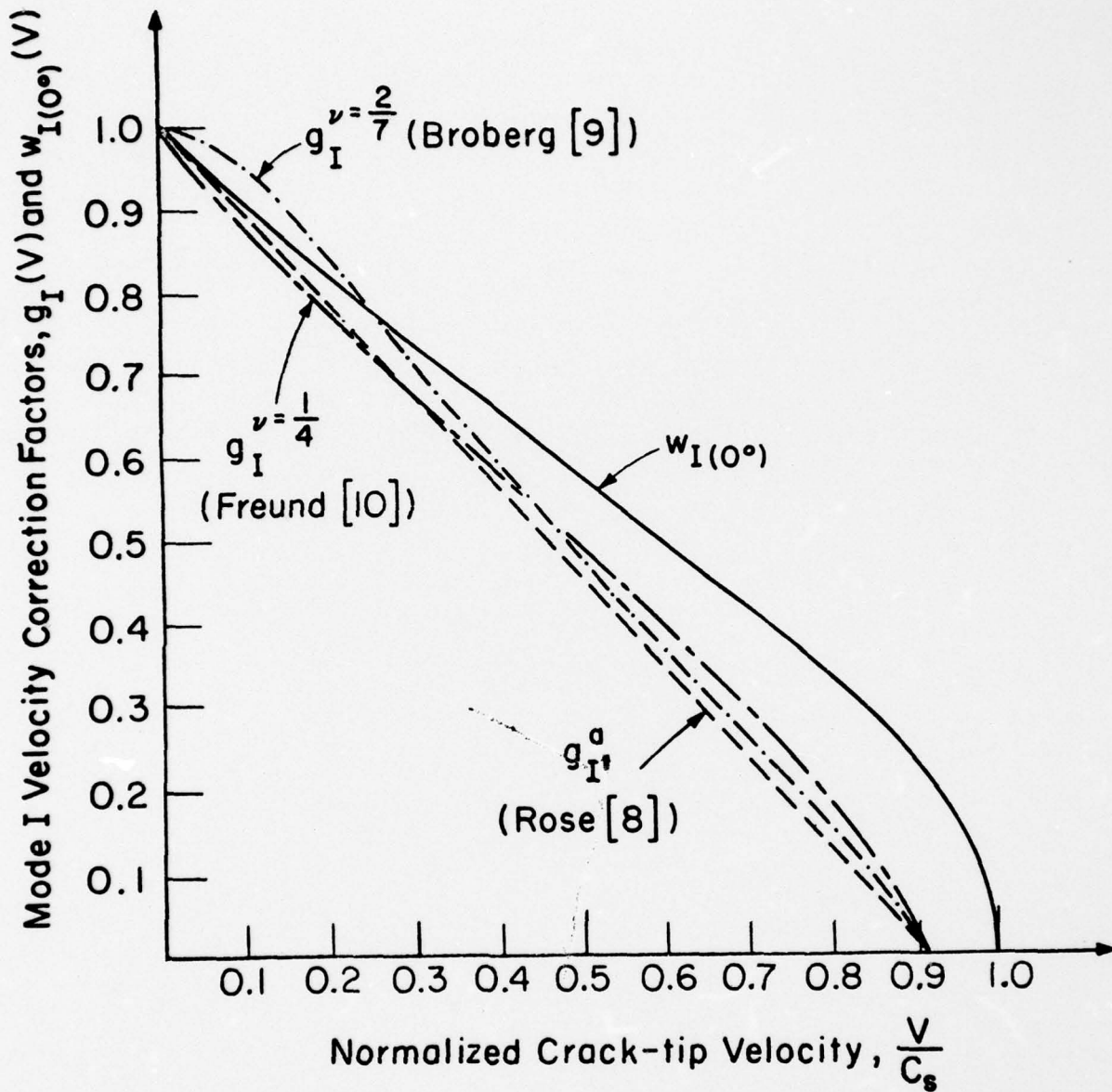
Fig. 3   Mode I velocity correction factors for homogeneous isotropic elastic materials (g_I^i) and for strongly orthotropic 0° unidirectional composites ($w_{I(0°)}$).

-37-

APPENDIX

The purpose of this appendix is to present the results of McClintock in greater detail than that which is given in [4]. Although the essential ideas and results are the same as those derived by McClintock and thus the credit for this analogy is his, we believe that the detailed presentation given herein provides additional delineation of the appli-cability of the analogy.

Order-of-Magnitude Approximations of Mode I Orthotropic (0°) Elastic Elastic Parameters

The strain (ε,γ) - stress (σ) relations in principal material coordinates for an orthotropic lamina under plane stress are [5]

$$\begin{Bmatrix} \varepsilon_{11} \\ \varepsilon_{22} \\ \gamma_{12} \end{Bmatrix} = \begin{bmatrix} a_{11} & a_{12} & 0 \\ a_{21} & a_{22} & 0 \\ 0 & 0 & a_{66} \end{bmatrix} \begin{Bmatrix} \sigma_{11} \\ \sigma_{22} \\ \sigma_{12} \end{Bmatrix} \qquad (A1)$$

where

$$a_{11} = \frac{1}{E_1} \qquad a_{22} = \frac{1}{E_2} \qquad a_{66} = \frac{1}{G_{12}}$$

$$a_{12} = a_{21} = -\frac{\nu_{12}}{E_1} = -\frac{\nu_{21}}{E_2} \ .$$

-39-

E_1 and E_2 are the extensional moduli in the x_1 and x_2 directions, respectively, G_{12} is the shear modulus in the x_1-x_2 plane, and the ν_{ij} are the Poisson's ratios for transverse strain in the j direction due to stress in the i direction. The Mode I orthotropic stress and displacement fields[†] are given in terms of the roots μ_i of the following equation [7]:

$$a_{11}\mu^4 + \left(2a_{12} + a_{66}\right)\mu^2 + a_{22} = 0 \tag{A2}$$

which has the solutions

$$\mu_1^2, \mu_2^2 = \frac{-\left(2a_{12} + a_{66}\right) \pm \left(2a_{12} + a_{66}\right)\sqrt{1 - \dfrac{4a_{11}a_{22}}{\left(2a_{12} + a_{66}\right)^2}}}{2a_{11}} . \tag{A3}$$

For a 0° graphite fiber composite (fibers extending along the x_2 direction), typical constitutive parameters give

$$\frac{E_2}{E_1} \approx 20 \qquad\qquad \frac{E_1}{G_{12}} \approx 2$$

$$\tag{A4}$$

$$\nu_{21} \approx \frac{1}{3} \qquad\qquad \nu_{12} \approx \frac{1}{60} .$$

Some simple combinations of the elastic constants will be evaluated for the purpose of order-of-magnitude approximations. Using eqns. (A1) and (A4)

[†]The explicit equations for these fields will be given later in this Appendix.

$$2a_{12} + a_{66} = -2 \frac{\nu_{12}}{E_1} + \frac{1}{G_{12}} \approx -\frac{1}{60G_{12}} + \frac{1}{G_{12}} \approx \frac{1}{G_{12}} = a_{66} \, . \qquad \text{(A5)}$$

Also,

$$4a_{11}a_{22} = 4 \frac{1}{E_1} \frac{1}{E_2} \approx \frac{4}{(E_1)(20E_1)} \approx \frac{1}{20G_{12}^2} \, . \qquad \text{(A6)}$$

Hence, from eqns. (A5) and (A6), it follows that

$$a_{66} \gg 2|a_{12}| \quad \text{and} \quad \left(2a_{12} + a_{66}\right)^2 \gg 4a_{11}a_{22} \, . \qquad \text{(A7)}$$

Observing that $\sqrt{1-\alpha}$ can be approximated by $1 - \frac{\alpha}{2}$ when $0 < \alpha \ll 1$, eqn. (A3) can be written as

$$\mu_1^2 \, , \mu_2^2 \approx \frac{-\left(2a_{12}+a_{66}\right) \pm \left(2a_{12}+a_{66}\right)\left[1 - \frac{1}{2}\frac{4a_{11}a_{22}}{\left(2a_{12}+a_{66}\right)^2}\right]}{2a_{11}}$$

which gives

$$\mu_1^2 \approx \frac{-2\left(2a_{12}+a_{66}\right)^2 + 2a_{11}a_{22}}{2a_{11}\left(2a_{12}+a_{66}\right)}$$

$$\mu_2^2 \approx -\frac{a_{22}}{\left(2a_{12}+a_{66}\right)} \, .$$
(A8)

By using the first condition in (A7) on μ_2^2 and both conditions in (A7) on μ_1^2, eqns. (A8) can be reduced further as

$$\mu_1^2 \approx -\frac{2a_{11} + a_{66}}{a_{11}} \approx -\frac{a_{66}}{a_{11}}$$

$$\mu_2^2 \approx -\frac{a_{22}}{2a_{12} + a_{66}} \approx -\frac{a_{22}}{a_{66}} . \tag{A9}$$

Also, the ratio of these roots is

$$\frac{\mu_1}{\mu_2} \approx \sqrt{\frac{a_{66}^2}{a_{11}a_{22}}} = \sqrt{\frac{E_1 E_2}{G_{12}^2}} \approx \sqrt{80} \approx 9 . \tag{A10}$$

Next, consider the complex variables z_1 and z_2 which are defined as

$$z_1 = \cos\theta + \mu_1 \sin\theta$$

$$z_2 = \cos\theta + \mu_2 \sin\theta \tag{A11}$$

where θ is the counterclockwise angle measured from the x_1 axis to r, thus forming an r, θ crack-tip polar coordinate system. Because μ_1 and μ_2 are pure imaginary quantities (Refer to eqn. (A9).), eqns. (A11) are

$$z_1 = \cos\theta + i|\mu_1|\sin\theta$$

$$z_2 = \cos\theta + i|\mu_2|\sin\theta \tag{A12}$$

-42-

which can be written as

$$z_1 = \left[\cos^2\theta + |\mu_1|^2 \sin^2\theta \right]^{1/2} e^{i\phi_1}$$

$$z_2 = \left[\cos^2\theta + |\mu_2|^2 \sin^2\theta \right]^{1/2} e^{i\phi_2}$$

(A13)

where the ϕ_i are

$$\phi_i = \tan^{-1} \frac{|\mu_i| \sin\theta}{\cos\theta} \ .$$

So,

$$\frac{z_1^{1/2}}{z_2^{1/2}} = \left[\frac{1 + \left(|\mu_1|^2 - 1\right)\sin^2\theta}{1 + \left(|\mu_2|^2 - 1\right)\sin^2\theta} \right]^{1/4} e^{\frac{i\left(\phi_1 - \phi_2\right)}{2}}$$

(A14)

which has a maximum when $\phi_{1,2} = \frac{\pi}{2}$ and $\theta = \frac{\pi}{2}$, and a minimum when $\phi_{1,2} = 0°$ and $\theta = 0°$. Thus,

$$\left(\frac{z_1^{1/2}}{z_2^{1/2}} \right)_{max} = \left(\frac{\mu_1}{\mu_2} \right)^{1/2} \quad \text{and} \quad \left(\frac{z_1^{1/2}}{z_2^{1/2}} \right)_{min} = 1 \ .$$

(A15)

Combining eqns. (A10) and (A15) gives the following maximum and minimum ratios:

-43-

$$
\left(\frac{\dfrac{\mu_1}{z_1^{1/2}}}{\dfrac{\mu_2}{z_2^{1/2}}} \right)_{\text{max.}} \approx 9
\qquad \text{and} \qquad
\left(\frac{\dfrac{\mu_1}{z_1^{1/2}}}{\dfrac{\mu_2}{z_2^{1/2}}} \right)_{\text{min.}} \approx 3
$$

$$\text{(A16)}$$

$$
\left(\frac{\dfrac{\mu_1}{z_2^{1/2}}}{\dfrac{\mu_2}{z_1^{1/2}}} \right)_{\text{max.}} \approx 27
\qquad \text{and} \qquad
\left(\frac{\dfrac{\mu_1}{z_2^{1/2}}}{\dfrac{\mu_2}{z_1^{1/2}}} \right)_{\text{min.}} \approx 9
$$

or, rewriting of eqns. (A16) gives

$$
\left(\frac{\mu_1}{z_1^{1/2}} \right) \approx (3 \text{ to } 9) \left(\frac{\mu_2}{z_2^{1/2}} \right)
$$

$$\text{(A17)}$$

$$
\left(\frac{\mu_1}{z_2^{1/2}} \right) \approx (9 \text{ to } 27) \left(\frac{\mu_2}{z_1^{1/2}} \right).
$$

-44-

Approximate Stress Fields for Mode I Orthotropic (0°) Composite

The singular crack-tip stress field is given by [7]

$$\sigma_{11} = \frac{k_1}{\sqrt{2r}} \quad Re\left[\frac{\mu_1\mu_2}{\mu_1-\mu_2}\left(\frac{\mu_2}{z_2^{1/2}} - \frac{\mu_1}{z_1^{1/2}}\right)\right]$$

$$\sigma_{22} = \frac{k_1}{\sqrt{2r}} \quad Re\left[\frac{1}{\mu_1-\mu_2}\left(\frac{\mu_1}{z_2^{1/2}} - \frac{\mu_2}{z_1^{1/2}}\right)\right] \qquad (A18)$$

$$\sigma_{12} = \frac{k_1}{\sqrt{2r}} \quad Re\left[\frac{\mu_1\mu_2}{\mu_1-\mu_2}\left(\frac{1}{z_1^{1/2}} - \frac{1}{z_2^{1/2}}\right)\right]$$

where k_1 is the stress intensity factor and Re denotes the real part of a complex function.

Recalling that $\left(\frac{\mu_1/z_1^{1/2}}{\mu_2/z_2^{1/2}}\right)$ is maximum ($\sim$9) for $\theta = 0°$ and minimum

($\sim$3) for $\theta = \frac{\pi}{2}$ and by letting $\mu_1 - \mu_2 \approx \mu_1$ in accordance with eqn. (A10), the first of eqns. (A18) may be written as

$$\sigma_{11} \approx \frac{k_1}{\sqrt{2r}} \quad Re\left[\frac{-\mu_1\mu_2}{z_1^{1/2}}\right] \qquad (A19)$$

-45-

where $\mu_2/z_2^{1/2}$ has been dropped in comparison with $\mu_1/z_1^{1/2}$. Substituting eqns. (A9) and (A11) into eqn. (A19) gives

$$\sigma_{11} \approx \frac{k_1}{\sqrt{2r}} \ \text{Re} \left[\frac{(-1)\left(i\sqrt{a_{66}/a_{11}}\right)\left(i\sqrt{a_{22}/a_{66}}\right)}{\left[\cos\theta + i\sqrt{a_{66}/a_{11}}\ \sin\theta\right]^{1/2}} \right]$$

or

$$\sigma_{11} \approx \frac{k_1}{\sqrt{2}} \ \text{Re} \left[\frac{\sqrt{a_{22}/a_{11}}}{\left(x_1 + i\sqrt{a_{66}/a_{11}}\ x_2\right)^{1/2}} \right] \tag{A20}$$

where $x_1 = r\cos\theta$ and $x_2 = r\sin\theta$ have been used. It is important to note that in deriving eqn. (A20), the requirement that $\mu_1/z_1^{1/2} \gg \mu_2/z_2^{1/2}$ has been used. This is true as $\theta \to 0°$. (As $\theta \to \frac{\pi}{2}$, $\mu_1/z_1^{1/2} \approx 3\left(\mu_2/z_2^{1/2}\right)$ which would result in about a 25% error in eqn. (A20) at $\theta = \frac{\pi}{2}$.) It is important to note that (1) σ_{11} is not used in the analogy for the derivation of the crack extension force and (2) for self-similar Mode I crack extension, the value of σ_{11} at $\theta = 0°$ would be the important value of σ_{11} if σ_{11} were used in a given analysis.

Recalling the second of eqns. (A17) and letting $\mu_1 - \mu_2 \approx \mu_1$, the second of eqns. (A18) may be written as

$$\sigma_{22} \approx \frac{k_1}{\sqrt{2r}} \ \text{Re} \left[\frac{1}{z_2^{1/2}} \right]$$

or using eqns. (A9) and (A11),

-46-

$$\sigma_{22} \approx \frac{k_1}{\sqrt{2}} \; \text{Re} \left[\frac{1}{\left(x_1 + i\sqrt{a_{22}/a_{66}} \; x_2 \right)^{1/2}} \right]. \qquad (A21)$$

From eqns. (A20) and (A21) it can be noted that along the x_1 axis (i.e., $x_2=0$),

$$\sigma_{22}/\sigma_{11} \approx \sqrt{a_{11}/a_{22}} \approx \sqrt{E_2/E_1} \approx 4.5.$$

Letting $\mu_1 - \mu_2 \approx \mu_1$, the third of eqns. (A18) becomes

$$\sigma_{12} \approx \frac{k_1}{\sqrt{2r}} \; \text{Re} \left[\frac{\mu_2}{z_1^{1/2}} - \frac{\mu_2}{z_2^{1/2}} \right]$$

or using eqns. (A9) and (A11),

$$\sigma_{12} \approx \frac{k_1}{\sqrt{2}} \; \text{Re} \left[\frac{i\sqrt{a_{22}/a_{66}}}{\left(x_1 + i\sqrt{a_{66}/a_{11}} \; x_2 \right)^{1/2}} - \frac{i\sqrt{a_{22}/a_{66}}}{\left(x_1 + i\sqrt{a_{22}/a_{66}} \; x_2 \right)^{1/2}} \right]. \qquad (A22)$$

Approximate Displacement Fields for Mode I Orthotropic (0°) Composite

The crack-tip displacement field is given by [7]

$$u_1 = k_1\sqrt{2r} \; \text{Re} \left[\frac{1}{\mu_1-\mu_2} \left(-p_1\mu_2 z_1^{1/2} + p_2\mu_1 z_2^{1/2} \right) \right]$$

$$\qquad (A23)$$

$$u_2 = k_1\sqrt{2r} \; \text{Re} \left[\frac{1}{\mu_1-\mu_2} \left(-q_1\mu_2 z_1^{1/2} + q_2\mu_1 z_2^{1/2} \right) \right]$$

-47-

where

$$p_i = a_{11}\mu_i^2 + a_{12} - a_{16}\mu_i$$

$$q_i = a_{12}\mu_i + \frac{a_{22}}{\mu_i} - a_{26}$$

where $a_{16} = a_{26} = 0$ for a 0° orthotropic composite. By letting $\mu_1 - \mu_2 \approx \mu_1$, eqns. (A23) become

$$u_1 \approx k_1\sqrt{2r}\ \mathrm{Re}\left[-p_1\frac{\mu_2}{\mu_1}z_1^{1/2} + p_2 z_2^{1/2}\right]$$

(A24)

$$u_2 \approx k_1\sqrt{2r}\ \mathrm{Re}\left[-q_1\frac{\mu_2}{\mu_1}z_1^{1/2} + q_2 z_2^{1/2}\right].$$

Examination of the first of eqns. (A24) gives

$$-p_1\frac{\mu_2}{\mu_1} = -\left[a_{11}\mu_1^2 + a_{12}\right]\left(\frac{\mu_2}{\mu_1}\right) \approx \left[a_{66} - a_{12}\right]\sqrt{\frac{a_{11}a_{22}}{a_{66}^2}}$$

where eqns. (A9) have been used for the μ_i. From the first condition in eqn. (A7), $a_{66} \gg |a_{12}|$, $-p_1\left(\frac{\mu_2}{\mu_1}\right) \approx \sqrt{a_{11}a_{22}}$.

(A25)

Further, using eqns. (A9) again gives

$$p_2 \approx a_{12} - \frac{a_{11}a_{22}}{a_{66}} \approx -\frac{1}{60E_1} - \frac{1}{40E_1}$$

(A26)

where the definitions of the a_{ij} (eqns. (A1)) and the typical constitutive parameters (eqns. (A4)) have been used. The first terms $\left(a_{12}, -\dfrac{1}{60E_1}\right)$ on each side of eqn. (A26) correspond to each other and the second terms $\left(-\dfrac{a_{11}a_{22}}{a_{66}}, -\dfrac{1}{40E_1}\right)$ on each side of eqn. (A26) correspond to each other. Thus, as eqn. (A26) indicates, a_{12} is not sufficiently larger than $a_{11}a_{22}/a_{66}$ to allow neglecting $a_{11}a_{22}/a_{66}$ in eqn. (A26). Therefore, substitution of eqns. (A25) and (A26) into (A24) gives

$$u_1 \approx k_1 \sqrt{2} \ \text{Re} \left[\sqrt{a_{11}a_{22}} \left(x_1 + \mu_1 x_2\right)^{1/2} + \left(a_{12} - \frac{a_{11}a_{22}}{a_{66}}\right)\left(x_1 + \mu_2 x_2\right)^{1/2} \right]. \qquad (A27)$$

Examination of the second of eqns. (A24) gives

$$q_1 \mu_2 z_1^{1/2} = \left(a_{12}\mu_1^2 + a_{22}\right)\left(\frac{\mu_2}{\mu_1}\right) z_1^{1/2} \approx \left(a_{22} - \frac{a_{12}a_{66}}{a_{11}}\right)\sqrt{\frac{a_{11}a_{22}}{a_{66}^2}} \ z_1^{1/2} \qquad (A28)$$

where eqns. (A9) have been used for the μ_i. From the definitions of the a_{ij} (eqns. (A1)) and the typical constitutive parameters (eqns. (A4)) note that

$$a_{22} \approx \frac{1}{40G_{12}} \qquad \text{and} \qquad -\frac{a_{12}a_{66}}{a_{11}} \approx \frac{1}{60G_{12}}$$

and therefore,

$$a_{22} \approx \frac{3}{2}\left(-\frac{a_{12}a_{66}}{a_{11}}\right). \qquad (A29)$$

Substitution of eqn. (A29) into eqn. (A28) gives

-49-

$$q_1\mu_2 z_1^{1/2} \approx -\frac{5}{2} a_{12}\sqrt{\frac{a_{22}}{a_{11}}} z_1^{1/2} .$$ (A30)

Also,

$$q_2\mu_1 z_2^{1/2} = \left(a_{12}\mu_2^2 + a_{22}\right)\left(\frac{\mu_1}{\mu_2}\right) z_2^{1/2} \approx a_{66}\sqrt{\frac{a_{22}}{a_{11}}} z_2^{1/2}$$ (A31)

where eqns. (A9) have used and the condition $a_{66} \gg |a_{12}|$ has been used. The ratio of eqn. (A31) to eqn. (A30) gives

$$\frac{q_2\mu_1 z_2^{1/2}}{-q_1\mu_2 z_1^{1/2}} \approx \left(\frac{2}{5}\right)\left(\frac{a_{66}}{a_{12}}\right)\left(\frac{z_2^{1/2}}{z_1^{1/2}}\right) \approx \left(\frac{2}{5}\right)(-120)\left(\frac{1}{3} \text{ to } 1\right)$$ (A32)

where eqns. (A1) and (A4) have been used to evaluate $\left(a_{66}/a_{12}\right)$ and eqns. (A10) and (A15) have been used to evaluate $\left(z_2^{1/2}/z_1^{1/2}\right)$. So,

$$\left|\frac{q_2\mu_1 z_2^{1/2}}{-q_1\mu_2 z_1^{1/2}}\right| \approx 16 \text{ to } 48.$$ (A33)

and thus, $\left|q_2\mu_1 z_2^{1/2}\right| \gg \left|q_1\mu_2 z_1^{1/2}\right|.$

Hence, the second of eqns. (A24) may be written as

$$u_2 \approx k_1\sqrt{2r} \, \text{Re}\left[\frac{1}{\mu_1} \, q_2\mu_1 z_2^{1/2}\right]$$ (A34)

-50-

where in accordance with eqn. (A33) the $q_1\mu_2 z_1^{1/2}$ term has been dropped. Therefore, by using eqns. (A9), eqn. (A34) becomes

$$u_2 \approx k_1\sqrt{2} \, \text{Re} \left[-i\sqrt{a_{66}a_{22}} \left(x_1 + i\sqrt{\frac{a_{22}}{a_{66}}} \, x_2 \right)^{1/2} \right] \tag{A35}$$

where as before, $x_1 = r\cos\theta$ and $x_2 = r\sin\theta$ have been used.

Analogy Between Mode III Isotropic (Exact) Fields and Mode I Orthotropic (Approximate) Fields

The crack-tip stress and displacement fields for the Mode III isotropic case are [7]

$$\sigma_{1'3'} = \frac{-k_{3'}}{\sqrt{2}} \, \text{Re} \left[\frac{i}{\left(x_{1'} + ix_{2'} \right)^{1/2}} \right] \tag{a}$$

$$\sigma_{2'3'} = \frac{k_{3'}}{\sqrt{2}} \, \text{Re} \left[\frac{1}{\left(x_{1'} + ix_{2'} \right)^{1/2}} \right] \tag{b} \text{(A36)}$$

$$u_{3'} = k_{3'}\sqrt{2} \, \text{Re} \left[-i\frac{1}{G} \left(x_{1'} + ix_{2'} \right)^{1/2} \right] \tag{c}$$

where the primed variables refer to the Mode III isotropic analysis. The paired variables to be investigated are

$$\sigma_{12} \text{ and } \sigma_{1'3'} \left[\text{eqn. (A22) and eqn. (A36-a)} \right]$$

-51-

σ_{22} and $\sigma_{2'3'}$ $\left[\text{eqn. (A21) and eqn. (A36-b)}\right]$

u_2 and $u_{3'}$ $\left[\text{eqn. (A35) and eqn. (A36-c)}\right]$.

Rewriting eqns. (A22) and (A36-a) gives

$$\sigma_{12} \approx \frac{k_1}{\sqrt{2}} \ \text{Re} \left[\frac{i\sqrt{a_{22}/a_{66}}}{\left(x_1 + i\sqrt{a_{66}/a_{11}}\, x_2\right)^{1/2}} - \frac{i\sqrt{a_{22}/a_{66}}}{\left(x_1 + i\sqrt{a_{22}/a_6}\, x_2\right)^{1/2}} \right] \quad (A22)$$

and

$$\sigma_{1'3'} = -\frac{k_{3'}}{\sqrt{2}} \ \text{Re} \left[\frac{i}{\left(x_{1'} + ix_{2'}\right)^{1/2}} \right] \quad (A36-a)$$

which indicate that if the first set of terms in the square brackets in eqn. (A22) were not present, a direct analogy between (A22) and (A36-a) would result.

As $x_1 \to 0$ for $x_2 \neq 0$, the first term in eqn. (A22) is smaller than the second term, and their ratio is

$$\left[\frac{\dfrac{i\sqrt{a_{22}/a_{66}}}{\left(x_1 + i\sqrt{a_{66}/a_{11}}\, x_2\right)^{1/2}}}{\dfrac{i\sqrt{a_{22}/a_{66}}}{\left(x_1 + i\sqrt{a_{22}/a_{66}}\, x_2\right)^{1/2}}} \right]_{x_1 \to 0} \approx \left(\frac{a_{22}/a_{66}}{a_{66}/a_{11}}\right)^{1/4} = \left(\frac{G_{12}^2}{E_1 E_2}\right)^{1/4} \approx \left(\frac{1}{80}\right)^{1/4} \approx \frac{1}{3} \quad (A37)$$

where eqns. (A1) and (A4) have been used. As $x_2 \to 0$ for $x_1 > 0$, (i.e., in front of the crack tip), both terms vanish and the difference is not important. As $x_2 \to 0$ for $x_1 < 0$, (i.e., along the crack flanks), the shear stress vanishes for all μ_1 .

As $x_2 \to 0$ for $x_1 > 0$, both σ_{12} and $\sigma_{1'3'}$ tend to zero in the same functional manner. So qualitatively, each term of eqn. (A22) behaves the same as $\sigma_{1'3'}$ does along the horizontal axis for $x_1 > 0$. Because the second term is three times larger than the first term in eqn. (A22), the first term will be neglected. However, as McClintock [4] observed, the neglection of the first term may not be justifiable, in general, because the first term reduces the magnitude of the shear stress above and below the crack tip, where the shear stress is maximum, by a factor of about two. Despite this general reservation regarding the shear stress σ_{12} , it poses no difficulty to the analysis presented in the body of this report because σ_{22} and u_2 along the horizontal axis are the only analogous quantities required. The reduced forms of eqn. (A22) and eqn. (A36-a) may be written respectively, as

$$\sigma_{12}\sqrt{\frac{a_{66}}{a_{22}}} \approx -\frac{k_1}{\sqrt{2}} \, \mathrm{Re} \left\{ \frac{i}{\left[x_1 + i\left(\sqrt{a_{22}/a_{66}}\, x_2\right) \right]^{1/2}} \right\} \tag{A38}$$

and

$$\sigma_{1'3'} = -\frac{k_{3'}}{\sqrt{2}} \, \mathrm{Re} \left[\frac{i}{\left(x_1' + ix_2' \right)^{1/2}} \right] \tag{A36-a}$$

from which the following analogies can be drawn:

$$\sigma_{1'3'} \longrightarrow \sigma_{12}\sqrt{\frac{a_{66}}{a_{22}}} = \sigma_{12}\sqrt{\frac{E_2}{G_{12}}}$$

$$k_{3'} \longrightarrow k_1$$

$$x_{1'} \longrightarrow x_1 \tag{A39}$$

$$x_{2'} \longrightarrow x_2\sqrt{\frac{a_{22}}{a_{66}}} = x_2\sqrt{\frac{G_{12}}{E_2}} \ .$$

Also, for eqns. (A21) and (A36-b)

$$\sigma_{22} \approx \frac{k_1}{\sqrt{2}} \ \text{Re} \left\{ \frac{1}{\left[x_1 + i\left(\sqrt{a_{22}/a_{66}} \ x_2 \right) \right]^{1/2}} \right\} \tag{A21}$$

and

$$\sigma_{2'3'} = \frac{k_{3'}}{\sqrt{2}} \ \text{Re} \left[\frac{1}{\left(x_{1'} + ix_{2'} \right)^{1/2}} \right] \tag{A36b}$$

from which the following analogies can be drawn:

$$\sigma_{2'3} \longrightarrow \sigma_{22}$$

$$k_{3'} \longrightarrow k_1 \quad \left(\sigma_{2'3'\infty}\sqrt{c'} \longrightarrow \sigma_{22\infty}\sqrt{c} \right)$$

$$x_{1'} \longrightarrow x_1 \tag{A40}$$

$$x_{2'} \longrightarrow x_2\sqrt{\frac{a_{22}}{a_{66}}} = x_2\sqrt{\frac{G_{12}}{E_2}}$$

where c' and c are the respective Mode III isotropic and Mode I orthotropic crack lengths. Thus, c'⟶c represents a useful analogy which follows directly from eqns. (A40). (This direct analogy between c' and c may be drawn from the direct analogy between $x_{1'}$ and x_1 also since the respective crack lengths simply represent specific lengths along the horizontal axes.) And, for eqns. (A35) and (A36-c)

$$u_2 \approx k_1 \sqrt{2} \; Re \left\{ -i \; \sqrt{a_{66}a_{22}} \; \left[x_1 + i \left(\sqrt{\frac{a_{22}}{a_{66}}} \; x_2 \right) \right]^{\frac{1}{2}} \right\} \tag{A35}$$

and

$$u_{3'} = k_3 \sqrt{2} \; Re \left[-i \; \frac{1}{G} \; \left(x_{1'} + ix_{2'} \right)^{\frac{1}{2}} \right] \tag{A36-c}$$

from which the following analogies can be drawn:

$$u_{3'} \longrightarrow u_2$$

$$k_{3'} \longrightarrow k_1$$

$$G \longrightarrow \frac{1}{\sqrt{a_{66}a_{22}}} = \sqrt{G_{12}E_2} \tag{A41}$$

$$x_{1'} \longrightarrow x_1$$

$$x_{2'} \longrightarrow x_2 \sqrt{\frac{a_{22}}{a_{66}}} = x_2 \sqrt{\frac{G_{12}}{E_2}}$$

It may be noted that eqns. (A39), (A40) and (A41) are consistent with each other including the definitions for k_1 and $k_{3'}$ which when expanded give

-55-

$$k_1 = \sigma_{22\infty}\sqrt{c} \quad \text{and} \quad k_{3'} = \sigma_{2'3'\infty}\sqrt{c'} \; .$$

Further Comments

1. Limit of Approximations –

The initial level of approximations which were used $\left(\text{i.e., } \mu_1^2 \approx -\dfrac{a_{66}}{a_{11}}\right.$ and $\left.\mu_2^2 \approx -\dfrac{a_{22}}{a_{66}}\right)$ can not be relaxed if the Mode III isotropic/Mode I orthotropic analogy is to remain applicable. If the more accurate, but still approximate, expressions $\mu_1^2 \approx -\dfrac{2a_{12} + a_{66}}{a_{11}}$ and $\mu_2^2 \approx -\dfrac{a_{22}}{2a_{12} + a_{66}}$ had been used (See eqn. (A9).), eqns. (A21), (A22) and (A35) would have become, respectively,

$$\sigma_{22} \approx \frac{k_1}{\sqrt{2}} \; \text{Re}\left\{\frac{1}{\left[x_1 + i\,\sqrt{a_{22}/(2a_{12} + a_{66})}\; x_2\right]^{1/2}}\right\}$$

$$\sigma_{12} \approx -\frac{k_1}{\sqrt{2}} \; \text{Re}\left\{\frac{i}{\left[x_1 + i\,\sqrt{a_{22}/(2a_{12} + a_{66})}\; x_2\right]^{1/2}}\right\} \qquad (A42)$$

$$u_2 \approx k_1\sqrt{2}\left\{-i\sqrt{\frac{a_{66}^2 a_{22}}{2a_{12} + a_{66}}}\;\left[x_1 + i\sqrt{a_{22}/(2a_{12} + a_{66})}\; x_2\right]^{1/2}\right\}.$$

-56-

If a check is made as to whether or not $\sigma_{2'3'} = G \dfrac{\partial u_{3'}}{\partial x_{2'}}$ results in

$\sigma_{22} = \dfrac{1}{a_{22}} \dfrac{\partial u_2}{\partial x_2}$ by analogy,[†] the following occurs:

$$\sigma_{22} = \sqrt{\frac{2a_{12} + a_{66}}{a_{22}a_{66}^2}} \ \ \frac{\partial u_2}{\partial \left[\sqrt{a_{22}/(2a_{12} + a_{66})} \ x_2\right]}$$

$$= \sqrt{\frac{2a_{12} + a_{66}}{a_{22}a_{66}^2}} \sqrt{\frac{2a_{12} + a_{66}}{a_{22}}} \ \ \frac{\partial u_2}{\partial x_2}$$

or,

$$\sigma_{22} = \frac{2a_{12} + a_{66}}{a_{66}} \cdot \frac{1}{a_{22}} \cdot \frac{\partial u_2}{\partial x_2} \ . \tag{A43}$$

In order to obtain the equation $\sigma_{22} = \dfrac{1}{a_{22}} \dfrac{\partial u_2}{\partial x_2}$, it is necessary to invoke

the further approximation that $a_{66} \gg 2|a_{12}|$, which is what has been used

throughout this appendix.

2.   Mode I Orthotropic $\sigma_{12} - \gamma_{12}$ Approximation -

   In order to insure the satisfaction of the $\sigma_{12} - \gamma_{12}$ equation in

accordance with the analogy, the constitutive equation $\sigma_{12} = G_{12}\left(\dfrac{\partial u_1}{\partial x_2} + \dfrac{\partial u_2}{\partial x_1}\right)$

[†]This is done in the main text of this report.

-57-

must consistently reduce to $\sigma_{12} \approx G_{12}\left(\dfrac{\partial u_2}{\partial x_1}\right)$. Recall from earlier in this appendix that

$$\sigma_{12} \approx \frac{k_1}{\sqrt{2}}\ \mathrm{Re}\left[\frac{i\sqrt{a_{22}/a_{66}}}{\left(x_1 + i\sqrt{a_{66}/a_{11}}\ x_2\right)^{1/2}} - \frac{i\sqrt{a_{22}/a_{66}}}{\left(x_1 + i\sqrt{a_{22}/a_{66}}\ x_2\right)^{1/2}}\right] \quad \text{(A22)}$$

and

$$\sigma_{1'3'} \approx -\frac{k_3}{\sqrt{2}}\ \mathrm{Re}\left[\frac{i}{\left(x_{1'} + ix_{2'}\right)^{1/2}}\right], \quad \text{(A36-a)}$$

and that arguments were provided to show that σ_{12} could be further reduced to

$$\sigma_{12} \approx -\frac{k_1}{\sqrt{2}}\ \mathrm{Re}\left[\frac{i\sqrt{a_{22}/a_{66}}}{\left(x_1 + i\sqrt{a_{22}/a_{66}}\ x_2\right)^{1/2}}\right]. \quad \text{(A38)}$$

In this discussion, it will be shown that dropping the first term in eqn. (A22) in order to obtain eqn. (A38) is essentially equivalent to dropping $\dfrac{\partial u_1}{\partial x_2}$ in the shear strain.

Note that

$$G_{12}\frac{\partial u_1}{\partial x_2} = \frac{1}{a_{66}}\ \frac{\partial u_1}{\partial x_2} \approx \frac{k_1}{\sqrt{2}}\ \mathrm{Re}\left[\frac{i\sqrt{a_{22}/a_{66}}}{\left(x_1 + i\sqrt{a_{66}/a_{11}}\ x_2\right)^{1/2}} - \frac{i\sqrt{a_{22}/a_{66}}\left(\dfrac{a_{11}a_{12}}{a_{66}^2} - \dfrac{a_{12}}{a_{66}}\right)}{\left(x_1 + i\sqrt{a_{22}/a_{66}}\ x_2\right)^{1/2}}\right] \quad \text{(A44)}$$

-58-

where eqns. (A27) and (A9) have been used. Also,

$$G_{12} \frac{\partial u_2}{\partial x_1} = \frac{1}{a_{66}} \frac{\partial u_2}{\partial x_1} \approx -\frac{k_1}{\sqrt{2}} \text{ Re} \left[\frac{i\sqrt{a_{22}/a_{66}}}{\left(x_1 + i\sqrt{a_{22}/a_{66}} \ x_2\right)^{\frac{1}{2}}} \right] \qquad (A45)$$

where eqn. (A35) has been used. Note that eqns. (A38) and (A45) are identical. However, eqn. (A44) cannot be discarded without a closer examination. The first term in eqn. (A44) is the same as the first term in eqn. (A22), which has been dropped in accordance with foregoing arguments. But the second term in eqn. (A44), except for the constant $\left(\dfrac{a_{11}a_{12}}{a_{66}^2} - \dfrac{a_{12}}{a_{66}} \right)$, is the same as eqn. (A45) which has been retained. Thus, in order to justify the discarding of the second term in eqn. (A44) also, it is necessary that

$$\left| \frac{a_{11}a_{12}}{a_{66}^2} - \frac{a_{12}}{a_{66}} \right| \ll 1 . \qquad (A46)$$

From eqns. (A1) and (A4)

$$\left(\frac{a_{11}a_{12}}{a_{66}^2} - \frac{a_{12}}{a_{66}} \right) = \left(\frac{\nu_{12}G_{12}}{E_1} - \frac{\nu_{12}G_{12}^2}{E_1^2} \right) \approx \frac{1}{240} \qquad (A47)$$

Thus, the necessary condition represented by the inequality (A46) is proved.

SECTION 3

GOVERNING EQUATIONS FOR MODE I DYNAMIC FRACTURE

IN ORTHOTROPIC DCB SPECIMENS WITH EXTERNAL

DYNAMIC INTERACTIONS

ABSTRACT

The governing partial differential equations for dynamic crack propagation in double cantilever beam (DCB) unidirectional composite specimens are derived. Only the Mode I symmetric case in which the loading is along a principal material axis and a self-similar crack propagates along the in-plane orthogonal principal material axis is considered. The natural dynamic interactive boundary conditions between the DCB specimen and the tensile testing machine are emphasized. A finite-difference solution scheme is presented.

INTRODUCTION

In the present study of the dynamic fracture of composite materials, one of the proposed experimental specimens is a double cantilever beam (DCB) which may be modeled as a Timoshenko beam on a generalized foundation. The composite material in the beam is modeled as a homogeneous orthotropic material and the analysis is restricted to the Mode I symmetric case in which the loading is along a principal material axis and a self-similar crack propagates along the in-plane orthogonal principal material axis. The analysis is similar to that by Kanninen [1] who derived analogous governing equations for a homogeneous isotropic DCB subjected to constant displacement loading.

In addition to the governing partial differential equations of the interior of the beam, the dynamic interactive boundary conditions between the DCB test specimen and the tensile testing machine are derived. Kousiounelos and Williams [2] considered the dynamic fracture DCB problem and derived the governing equations but did not consider interactive boundary conditions. For completeness, the derivation of the governing partial differential equations will be presented here as well as the derivation of the natural boundary conditions which account for the dynamic interaction between the test specimen and the tensile testing machine.

EQUATIONS OF MOTION AND BOUNDARY CONDITIONS

The structure to be analyzed is shown in Fig. 1. From Fig. 1b it can be seen that there are two regions of the beam where different equations of motion are applicable. These are the cracked region where no elastic foundation exists and the uncracked region where a generalized foundation is present. In deriving the equations of motion for both of these regions, the singularity function $\langle x-a \rangle^\circ$ which is zero for negative values in the brackets and is unity otherwise will be used. A variational derivation of the equations of motion will be presented.

The variational indicator for Hamilton's principle is [3]

$$\text{V.I.} = \int_{t_1}^{t_2} \left[\delta(T^* - V) + \sum_{j=1}^{n} \Xi_j \delta \eta_j \right] dt \tag{1}$$

where t is time, η_j are the generalized coordinates, and Ξ_j are the generalized forces corresponding to the nonconservative forces. The kinetic coenergy (T^*) and the potential energy (V) functionals are given by

$$T^* = \int_0^L \left\{ \frac{1}{2} \rho A \left(\frac{\partial w}{\partial t} \right)^2 + \frac{1}{2} \rho I \left(\frac{\partial \psi}{\partial t} \right)^2 \right\} dx + \frac{1}{2} m \left[\frac{\partial w(0,t)}{\partial t} \right]^2 \tag{2}$$

$$V = \int_0^L \left\{ \frac{1}{2} E_1 I \left(\frac{\partial \psi}{\partial x} \right)^2 + \frac{1}{2} \kappa G_{12} A \left(\frac{\partial w}{\partial x} - \psi \right)^2 \right.$$

$$\left. + \langle x-a \rangle^\circ \frac{1}{2} \left(k_e w^2 + k_r \psi^2 \right) \right\} dx + \frac{1}{2} k_s \left[w(0,t) - \dot{w}_o t \right]^2 \tag{3}$$

-65-

The generalized coordinates are w, the transverse displacement, and ψ, the in-plane rotation. The beam has mass density ρ, cross-sectional area A, flexural moment of inertia I, and shear coefficient κ. E_1 is the extensional modulus in the 1 direction and G_{12} is the shear modulus in the 1-2 plane, as indicated in Fig. 1. k_e and k_r are the extensional and rotational foundation stiffnesses, respectively. The crack tip is at $x = a(t)$. Because the crack tip cannot "heal", if at any value of x the function $<x-a>^\circ$ is zero, this function cannot become unity at any later time. It is assumed that the beam contains negligible structural damping and that no nonconservative forces act on the system; thus the Ξ_j are zero. The tensile testing machine interactions are modeled in Fig. 2 where an extensional spring with spring constant k_s and a translational mass m represent the machine's stiffness and inertia, respectively. The cross-head of the testing machine is assumed to move at a constant displacement rate, thus one end of the spring k_s is assumed to move at a constant velocity $\dot{w}_o$.

Substitution of eqns. (2) and (3) into eqn. (1) and use of the calculus of variations give

$$V.I. = \int_{t_1}^{t_2} dt \left\{ \int_0^L dx \left[-\rho A \frac{\partial^2 w}{\partial t^2} + \kappa G_{12} A \left(\frac{\partial^2 w}{\partial x^2} - \frac{\partial \psi}{\partial x} \right) - <x-a>^\circ k_e w \right] \delta w(x,t) \right.$$

$$+ \int_0^L dx \left[-\rho I \frac{\partial^2 \psi}{\partial t^2} + E_1 I \frac{\partial^2 \psi}{\partial x^2} + \kappa G_{12} A \left(\frac{\partial w}{\partial x} - \psi \right) - <x-a>^\circ k_r \psi \right] \delta \psi(w,t)$$

$$+ \left[-E_1 I \frac{\partial \psi(L,t)}{\partial x} \right] \delta \psi(L,t) + \left[E_1 I \left(\frac{\partial \psi(0,t)}{\partial x} \right) \right] \delta \psi(0,t)$$

(equation continued)

-66-

$$+ \left[-\kappa G_{12}A \left(\frac{\partial w(L,t)}{\partial x} - \psi(L,t) \right) \right] \delta w(L,t)$$

$$+ \left[-m \frac{\partial^2 w(0,t)}{\partial t^2} + \kappa G_{12}A \left(\frac{\partial w(0,t)}{\partial x} - \psi(0,t) \right) - k_s \left(w(0,t) - \dot{w}_o t \right) \right] \delta w(0,t) \Bigg\}. \quad (4)$$

The necessary conditions for the variational indicator in eqn. (4) to vanish for arbitrary admissible variations of w and ψ are

$$\left. \begin{array}{l} \kappa G_{12}A \left(\dfrac{\partial^2 w}{\partial x^2} - \dfrac{\partial \psi}{\partial x} \right) - \langle x-a \rangle^o k_e w = \rho A \dfrac{\partial^2 w}{\partial t^2} \\[4mm] E_1 I \dfrac{\partial^2 \psi}{\partial x^2} + \kappa G_{12}A \left(\dfrac{\partial w}{\partial x} - \psi \right) - \langle x-a \rangle^o k_r \psi = \rho I \dfrac{\partial^2 \psi}{\partial t^2} \end{array} \right\} \quad 0 < x < L \qquad (5)$$

and

$$\left. \begin{array}{l} E_1 I \dfrac{\partial \psi(0,t)}{\partial x} = 0 \\[6mm] m \dfrac{\partial^2 w(0,t)}{\partial t^2} + k_s \left(w(0,t) - \dot{w}_o t \right) = \kappa G_{12}A \left(\dfrac{\partial w(0,t)}{\partial x} - \psi(0,t) \right) \end{array} \right\} \text{at } x=0 \quad (6)$$

$$\left. \begin{array}{l} E_1 I \dfrac{\partial \psi(L,t)}{\partial x} = 0 \\[6mm] \kappa G_{12}A \left(\dfrac{\partial w(L,t)}{\partial x} - \psi(L,t) \right) = 0 \end{array} \right\} \text{at } x=L . \qquad (7)$$

Eqns. (5) are the partial differential equations of motion and eqns. (6) and (7) are the natural boundary conditions. In deriving eqns. (5), (6) and (7) it has been assumed that E_1, G_{12}, A, I, k_e and k_r are independent of x and t.

FOUNDATION PARAMETERS

The elastic foundation parameters represent the effects of the extensional and bending forces transmitted across the uncracked plane of the specimen. The model which is used is shown in Fig. 3. From Fig. 3(b), the extensional equilibrium, compatibility and constitutive relations are, respectively,

$$\sigma_y b = k_e w(x)$$

$$\epsilon_y = \frac{2w(x)}{h} \tag{8}$$

$$\sigma_y = E_2 \epsilon_y$$

where σ_y and ϵ_y are the extensional stress and strain in the y direction and E_2 is the associated extensional modulus. Combining the relations in (8) gives

$$k_e = \frac{2E_2 b}{h} . \tag{9}$$

From Fig. 3(c), the rotational equilibrium, compatibility and constitutive relations are, respectively,

$$\left(\tau_{yx}\right)_{Avg.} b \frac{h}{2} = k_r \psi(x)$$

$$\left(\gamma_{yx}\right)_{Avg.} = \psi(x) \tag{10}$$

$$\left(\tau_{yx}\right)_{Avg.} = \kappa G_{12} \left(\gamma_{yx}\right)_{Avg.}$$

where $\left(\tau_{yx}\right)_{Avg.}$ and $\left(\gamma_{yx}\right)_{Avg.}$ are the space-averaged shear stress and strain, respectively. Combining the relations in (10) gives

$$k_r = \frac{\kappa G_{12} A}{2} .$$

(11)

CRACK PROPAGATION ENERGY CRITERION

In developing the crack propagation energy criterion, it is assumed that heat generation and heat propagation effects are negligible throughout the body and that the body remains linearly elastic except for a small undefined crack-tip region in which the fracture process is occurring. So, by the conservation of mechanical energy, the incremental energy absorbed by the extending crack must be equal to the incremental work done on the system minus the incremental mechanical energy released by the system. Thus, for a given increment of crack advance da, this may be expressed as

$$Rb \, da = d\mathscr{W} - d\mathscr{E} \tag{12}$$

or

$$Rb = \left(\frac{d\mathscr{W}}{dt} - \frac{d\mathscr{E}}{dt}\right)\frac{dt}{da} \tag{13}$$

where R is the dynamic fracture toughness of the composite, $\mathscr{W}$ is total external work done on the specimen by both the upper and lower machine loadings, and $\mathscr{E}$ is the total mechanical energy in the system containing both halves of the DCB specimen as well as both the upper and lower testing machine elements.

The total mechanical energy in the system is

$$\mathscr{E} = T_T + V_T \tag{14}$$

where T_T and V_T are the total kinetic and total potential energies, respectively. Because the system is linear

$$T_T = 2T^* \quad \text{and} \quad V_T = 2V \tag{15}$$

-71-

where T^* and V are defined in eqns. (2) and (3). So,

$$\frac{d\mathscr{E}}{dt} = 2\frac{dT^*}{dt} + 2\frac{dV}{dt} . \tag{16}$$

Substituting eqns. (2) and (3) into eqn. (16), and performing the differentiation indicated in eqn. (16) give

$$\frac{d\mathscr{E}}{dt} = 2\int_0^L \frac{\partial\psi}{\partial t}\left\{\rho I\frac{\partial^2\psi}{\partial t^2} - E_1 I\frac{\partial^2\psi}{\partial x^2} - \kappa G_{12}A\left(\frac{\partial w}{\partial x} - \psi\right) + <x-a>^\circ k_r\psi\right\}dx$$

$$+ 2\int_0^L \frac{\partial w}{\partial t}\left\{\rho A\frac{\partial^2 w}{\partial t^2} - \kappa G_{12}A\left(\frac{\partial^2 w}{\partial x^2} - \frac{\partial\psi}{\partial x}\right) + <x-a>^\circ k_e w\right\}dx$$

$$- 2k_s\left[w(0,t) - \dot{w}_o t\right]\dot{w}_o + \left.\left(k_e w^2 + k_r\psi^2\right)\right|_{x=a}\left(-\frac{da}{dt}\right) \tag{17}$$

where the boundary conditions represented by eqns. (6) and (7) have been used in reducing eqn. (17) to the form given. By eqns. (5), the flower brackets in eqn. (17) vanish, and thus eqn. (17) reduces to

$$\frac{d\mathscr{E}}{dt} = -2k_s\left[w(0,t) - \dot{w}_o t\right]\dot{w}_o - \frac{da}{dt}\left.\left(k_e w^2 + k_r\psi^2\right)\right|_{x=a} . \tag{18}$$

The work done on the system is input via the testing machine stiffness by the constant velocity $\dot{w}_o$. (Refer to Fig. 2.) The upward force in the machine's compliance is $k_s\left[\dot{w}_o t - w(0,t)\right]$. So, the total work increment is

$$d\mathscr{W} = 2k_s\left[\dot{w}_o t - w(0,t)\right]dw_o \tag{19}$$

-72-

from which

$$\frac{d\mathscr{W}}{dt} = 2k_s\left[\dot{w}_o t - w(0,t)\right]\dot{w}_o \ . \tag{20}$$

Substitution of eqns. (18) and (20) into eqn. (13) gives

$$Rb = \left(k_e w^2 + k_r \psi^2\right)\Big|_{x=a} \ . \tag{21}$$

Using the dynamic surface fracture energy γ_d, eqn. (21) may be written as

$$\gamma_d = \frac{1}{2b}\left[k_e w^2 + k_r \psi^2\right]_{x=a} \tag{22}$$

where the definition $R = 2\gamma_d$ has been used. Further, these results can be expressed in terms of the dynamic crack extension force $\mathscr{G}_d$[†] by noting that

$$\mathscr{G}_d \equiv \frac{1}{b}\left[\frac{d\mathscr{W}}{da} - \frac{d\mathscr{E}}{da}\right] \tag{23}$$

which may be rewritten as

$$\mathscr{G}_d = \frac{1}{b}\left[k_e w^2 + k_r \psi^2\right]_{x=a} \tag{24}$$

where k_e and k_r are given in eqns. (9) and (11), respectively.

[†] $\mathscr{G}_d$ is also called the dynamic energy release rate.

-73-

NONDIMENSIONAL EQUATIONS

In preparation for solving the governing equations it is convenient to nondimensionalize the equations of motion and the boundary conditions. If

$$\theta_c \equiv bR \quad \text{and} \quad \theta \equiv k_e w^2 + k_r \psi^2, \tag{25}$$

the singularity condition $\langle x-a \rangle^\circ$ can be restated as $\langle \theta_c - \theta \rangle^\circ$. Also, it is convenient to define the following nondimensional variables:

$$\zeta = \frac{x}{h} \quad ; \quad \tau = \sqrt{\frac{E_1}{12\rho}} \ \frac{t}{h}$$

$$W = w \sqrt{\frac{k_e}{\theta_c}} \quad ; \quad Y = h\psi \sqrt{\frac{k_e}{\theta_c}} \tag{26}$$

$$\dot{W}_o = \dot{w}_o \sqrt{\frac{k_e}{\theta_c}} \bigg/ \left(\sqrt{\frac{E_1}{12\rho}} \ \frac{1}{h} \right).$$

Substitution of eqns. (26) into the first of eqns. (5) gives

$$\frac{12\kappa G_{12}}{E_1} \left[\frac{\partial^2 W}{\partial \zeta^2} - \frac{\partial Y}{\partial \zeta} \right] - \langle \theta_c - \theta \rangle^\circ \ \frac{12h^2 k_e}{AE_1} \ W = \frac{\partial^2 W}{\partial \tau^2} . \tag{27}$$

Substitution of eqns. (26) into the second of eqns. (5) gives

$$\frac{\partial^2 Y}{\partial \zeta^2} + \frac{\kappa G_{12} A h^2}{E_1 I} \left[\frac{\partial W}{\partial \zeta} - Y \right] - \langle \theta_c - \theta \rangle^\circ \ \frac{k_r h^2}{E_1 I} Y = \frac{1}{12} \frac{\partial^2 Y}{\partial \tau^2} . \tag{28}$$

If the DCB has a constant rectangular cross section such that

-75-

$$A = bh \qquad I = \frac{bh^3}{12} \qquad \kappa = \frac{5}{6}$$

$$\qquad (29)$$

$$k_e = \frac{2E_2 b}{h} \qquad\qquad k_r = \frac{5}{12} G_{12} bh,$$

eqns. (27) and (28) become, respectively,

$$\frac{\partial^2 W}{\partial \zeta^2} - \frac{\partial Y}{\partial \zeta} - \langle \theta_c - \theta \rangle^\circ \frac{12E_2}{5G_{12}} W = \frac{E_1}{10G_{12}} \frac{\partial^2 W}{\partial \tau^2} \qquad (30)$$

and

$$\frac{\partial^2 Y}{\partial \zeta^2} + \frac{10G_{12}}{E_1} \left(\frac{\partial W}{\partial \zeta} - Y \right) - \langle \theta_c - \theta \rangle^\circ \frac{5G_{12}}{E_1} Y = \frac{1}{12} \frac{\partial^2 Y}{\partial \tau^2} \quad . \qquad (31)$$

Also, if eqns. (26) are substituted into the natural boundary conditions, eqns. (6) and (7) become, respectively,

$$\left. \begin{array}{l} \dfrac{\partial Y(0,\tau)}{\partial \zeta} = 0 \\[2em] \dfrac{m}{h^2} \left(\dfrac{E_1}{12\rho} \right) \dfrac{\partial^2 W(0,\tau)}{\partial \tau^2} + k_s \left[W(0,\tau) - \dot{W}_o \tau \right] \\[2em] \qquad\qquad = \kappa G_{12} A \, \dfrac{1}{h} \left[\dfrac{\partial W(0,\tau)}{\partial \zeta} - Y(0,\tau) \right] \end{array} \right\} \text{ at } \zeta = 0 \qquad (32)$$

and

$$\left. \begin{array}{l} \dfrac{\partial Y\left(\frac{L}{h},\tau\right)}{\partial \zeta} = 0 \\[2em] \dfrac{\partial W\left(\frac{L}{h},\tau\right)}{\partial \zeta} - Y\left(\frac{L}{h},\tau\right) = 0 \end{array} \right\} \text{ at } \zeta = \frac{L}{h} . \qquad (33)$$

-76-

An important part of the dynamic fracture computation is the evaluation of the energy and work expressions during crack propagation. Substitution of eqns. (26) into eqn. (2) gives

$$\frac{2T^*}{RA} = \frac{1}{24} \frac{E_1}{E_2} \left\{ \int_0^{L/h} \left[\left(\frac{\partial W}{\partial \tau}\right)^2 + \frac{1}{12} \left(\frac{\partial Y}{\partial \tau}\right)^2 \right] d\zeta + \frac{m}{\rho hA} \left(\frac{\partial W(0,\tau)}{\partial \tau}\right)^2 \right\} . \quad (34)$$

Substitution of eqns. (26) into eqn. (3) gives

$$\frac{2V}{RA} = \int_0^{L/h} \left[\frac{1}{24} \frac{E_1}{E_2} \left(\frac{\partial Y}{\partial \zeta}\right)^2 + \frac{5}{12} \frac{G_{12}}{E_2} \left(\frac{\partial W}{\partial \zeta} - Y\right)^2 \right.$$

$$\left. + \langle\theta_c - \theta\rangle^\circ \left(W^2 + \frac{5}{24} \frac{G_{12}}{E_2} Y^2\right) \right] d\zeta + \frac{k_s}{2E_2 b} \left[W(0,\tau) - \dot{W}_o \tau \right]^2 . \quad (35)$$

Substitution of eqns. (26) into eqn. (19) gives

$$\frac{\mathscr{W}}{RA} = \frac{k_s}{E_2 b} \left[\dot{W}_o \tau - W(0,\tau) \right] \dot{W}_o \tau . \qquad (36)$$

FINITE-DIFFERENCE SOLUTION SCHEME

Equations (30) and (31) may be written in their respective finite-difference formulations as

$$\frac{1}{(\Delta\zeta)^2}\left\{W(\zeta+\Delta\zeta,\ \tau) - 2W(\zeta,\tau) + W(\zeta-\Delta\zeta,\ \tau)\right\}$$

$$- \frac{1}{2\Delta\zeta}\left\{Y(\zeta+\Delta\zeta,\ \tau) - Y(\zeta-\Delta\zeta,\ \tau)\right\} - <\theta_c-\theta>^\circ\ \frac{12E_2}{5G_{12}}\ W(\zeta,\tau)$$

$$= \frac{E_1}{10G_{12}(\Delta\tau)^2}\left\{W(\zeta,\ \tau+\Delta\tau) - 2W(\zeta,\tau) + W(\zeta,\tau-\Delta\tau)\right\} \qquad (37)$$

and

$$\frac{1}{(\Delta\zeta)^2}\left\{Y(\zeta+\Delta\zeta,\ \tau) - 2Y(\zeta,\tau) + Y(\zeta-\Delta\zeta,\ \tau)\right\}$$

$$+ \frac{5G_{12}}{E_1(\Delta\zeta)}\left\{W(\zeta+\Delta\zeta,\ \tau) - W(\zeta-\Delta\zeta,\ \tau)\right\} - \frac{5G_{12}}{E_1}\left[2 + <\theta_c-\theta>^\circ\right]Y(\zeta,\tau)$$

$$= \frac{1}{12(\Delta\tau)^2}\left\{Y(\zeta,\ \tau+\Delta\tau) - 2Y(\zeta,\tau) + Y(\zeta,\ \tau-\Delta\tau)\right\} \qquad (38)$$

where Δ is the incremental finite-difference operator. Solving eqn. (37) for $W(\zeta,\ \tau+\Delta\tau)$ gives

$$W(\zeta,\ \tau+\Delta\tau) = \frac{10G_{12}}{E_1}\left(\frac{\Delta\tau}{\Delta\zeta}\right)^2\left\{W(\zeta+\Delta\zeta,\ \tau) + W(\zeta-\Delta\zeta,\ \tau)\right\}$$

$$-\frac{5G_{12}}{E_1}\frac{(\Delta\tau)^2}{\Delta\zeta}\left\{Y(\zeta+\Delta\zeta,\ \tau) - Y(\zeta-\Delta\zeta,\ \tau)\right\}$$

$$-\left\{\frac{20G_{12}}{E_1}\left(\frac{\Delta\tau}{\Delta\zeta}\right)^2 - 2 + 24\ \frac{E_2}{E_1}\ (\Delta\tau)^2<\theta_c-\theta>°\right\}W(\zeta,\tau)$$

$$- W(\zeta,\ \tau-\Delta\tau). \tag{39}$$

Solving eqn. (38) for $Y(\zeta,\ \tau+\Delta\tau)$ gives

$$Y(\zeta,\ \tau+\Delta\tau) = 12\left(\frac{\Delta\tau}{\Delta\zeta}\right)^2\left\{Y(\zeta+\Delta\zeta,\ \tau) + Y(\zeta-\Delta\zeta,\ \tau)\right\}$$

$$+\frac{60G_{12}}{E_1}\frac{(\Delta\tau)^2}{\Delta\zeta}\left\{W(\zeta+\Delta\zeta,\ \tau) - W(\zeta-\Delta\zeta,\ \tau)\right\}$$

$$-\left\{24\left(\frac{\Delta\tau}{\Delta\zeta}\right)^2 - 2 + 60\ \frac{G_{12}}{E_1}\ (\Delta\tau)^2\left[2 + <\theta_c-\theta>°\right]\right\}Y(\zeta,\tau)$$

$$- Y(\zeta,\ \tau-\Delta\tau). \tag{40}$$

-80-

Eqns. (39) and (40) are the recursion relations to be used in the computations. The associated boundary conditions may be written by expressing eqns. (32) and (33) in their respective finite-difference formulations as

$$Y(-\Delta\zeta, \tau) = Y(\Delta\zeta, \tau)$$

$$\left. W(0, \tau+\Delta\tau) = \frac{(\Delta\tau)^2}{\frac{m}{h^2}\left(\frac{E_1}{12\rho}\right)} \left\{ \kappa G_{12} A \frac{1}{h} \left[\frac{W(\Delta\zeta, \tau) - W(-\Delta\zeta, \tau)}{2\Delta\zeta} - Y(0, \tau) \right] \right.$$

$$\left. - k_s \left[W(0, \tau) - \dot{W}_o \tau \right] - W(0, \tau-\Delta\tau) \right\} \quad \text{at } \zeta = 0 \quad (41)$$

$$+ 2W(0, \tau)$$

and

$$\left. \begin{array}{l} Y\left(\dfrac{L}{h} + \Delta\zeta, \tau\right) = Y\left(\dfrac{L}{h} - \Delta\zeta, \tau\right) \\[2ex] W\left(\dfrac{L}{h} + \Delta\zeta, \tau\right) = W\left(\dfrac{L}{h} - \Delta\zeta, \tau\right) + 2\Delta\zeta Y\left(\dfrac{L}{h}, \tau\right) \end{array} \right\} \quad \text{at } \zeta = \frac{L}{h} . \quad (42)$$

Further, the initial conditions can be obtained by solving the static problem of a Timoshenko beam on an elastic foundation for the loading conditions at $\tau = 0$.

From eqn. (34) and by using backward differences for the time derivatives, the kinetic coenergy may be written as

$$
\frac{2T^*}{RA} = \frac{1}{24} \frac{E_1}{E_2} \sum_{\substack{\text{Over Beam} \\ \text{Length}}} \left\{ \left[\frac{3W(\zeta,\tau) - 4W(\zeta, \tau-\Delta\tau) + W(\zeta, \tau-2\Delta\tau)}{2\Delta\tau} \right]^2 \right.
$$

$$
+ \frac{1}{12} \left[\frac{3Y(\zeta,\tau) - 4Y(\zeta, \tau-\Delta\tau) + Y(\zeta, \tau-2\Delta\tau)}{2\Delta\tau} \right]^2 \right\} \Delta\zeta
$$

$$
+ \frac{1}{12} \frac{E_1}{E_2} \frac{m}{\rho hA} \left[\frac{3W(0,\tau) - 4W(0, \tau-\Delta\tau) + W(0, \tau-2\Delta\tau)}{2\Delta\tau} \right]^2 . \quad (43)
$$

Similarly, from eqn. (35) and by using central differences for the spatial derivatives, the potential energy may be written as

$$
\frac{2V}{RA} = \sum_{\substack{\text{Over Beam} \\ \text{Length}}} \left\{ \frac{1}{24} \frac{E_1}{E_2} \left[\frac{Y(\zeta+\Delta\zeta, \tau) - Y(\zeta-\Delta\zeta, \tau)}{2\Delta\zeta} \right]^2 \right.
$$

$$
+ \frac{5}{12} \frac{G_{12}}{E_2} \left[\frac{W(\zeta+\Delta\zeta, \tau) - W(\zeta-\Delta\zeta, \tau)}{2\Delta\zeta} - Y(\zeta,\tau) \right]^2
$$

$$
+ <\theta_c - \theta>^° \left[W^2(\zeta,\tau) + \frac{5}{24} \frac{G_{12}}{E_2} Y^2(\zeta,\tau) \right] \right\} \Delta\zeta
$$

$$
+ \frac{k_s}{2E_2 b} \left[W(0,\tau) - \dot{W}_o \tau \right]^2 . \quad (44)
$$

The corresponding finite-difference equation for the work expression is identical to eqn. (36). Further, it is noted that the forms of eqns. (43)

-82-

and (44) are written differently so as to ensure that the approximate errors in each are of the same order.

It is necessary to establish an integration step size in order to perform the above finite-difference calculations. A thorough error analysis of the governing differential equations [that is, eqns. (30) and (31)] provides the following restrictions [4]:

$$\frac{\Delta\tau}{\Delta\zeta} \leq \sqrt{\frac{E_1}{10G_{12}}}$$

and,

(45)

$$\frac{\Delta\tau}{\Delta\zeta} \leq \sqrt{\frac{1}{12}}$$

where the appropriate $\frac{\Delta\tau}{\Delta\zeta}$ is the smaller of the two.

REFERENCES

1. M.F. Kanninen, "A Dynamic Analysis of Unstable Crack Propagation and Arrest in the DCB Test Specimen", International Journal of Fracture, Vol. 10, No. 3, September 1974, pp. 415-430.

2. P.N. Kousiounelos and J.H. Williams, Jr., "Governing Equations for Dynamic Crack Propagation in DCB Unidirectional Composite Specimens", Composite Materials and Nondestructive Evaluation Laboratory, M.I.T., November 1977.

3. S.H. Crandall et al., Dynamics of Mechanical and Electromechanical Systems, McGraw-Hill Book Co., New York, 1968.

4. "Numerical Stability and Convergence Criteria for Equations for Dynamic Fracture in DCB Composite Specimens," Section 4 of this Report.
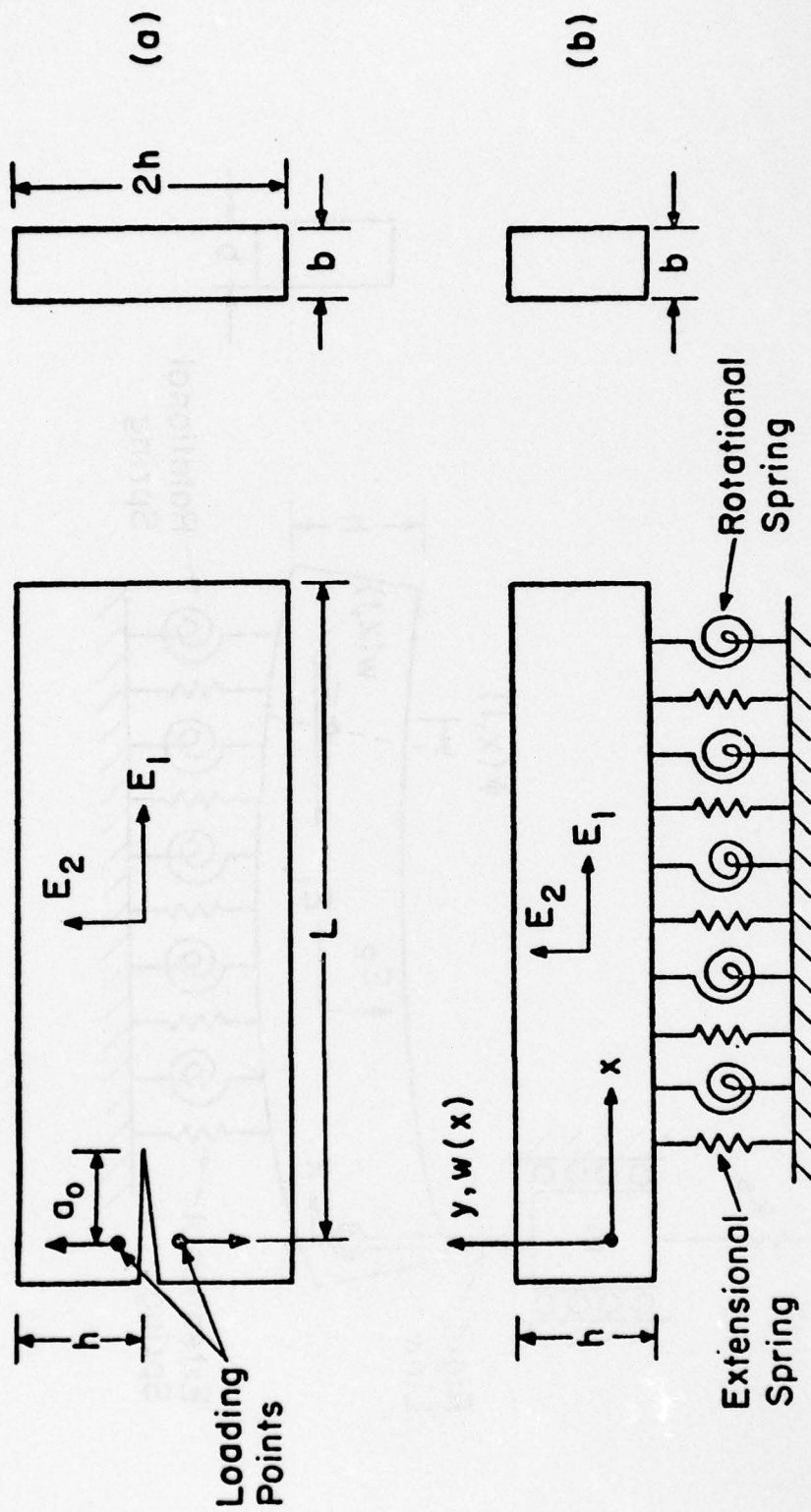
Fig. 1   Orthotropic double cantilever beam (ODCB) a) specimen and
          b) dynamic model.
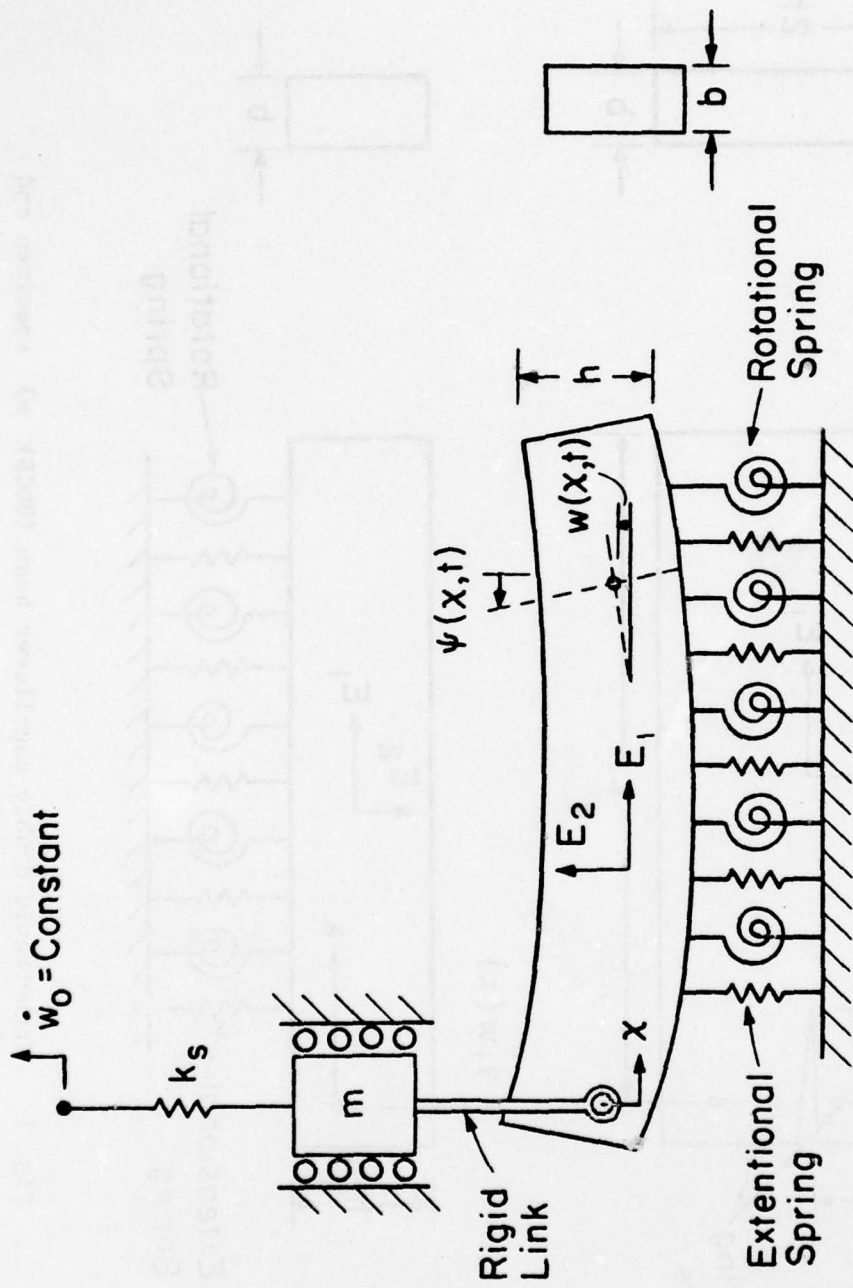
Fig. 2   Dynamic model of the orthotropic DCB specimen with the accompanying tensile machine stiffness and inertia.
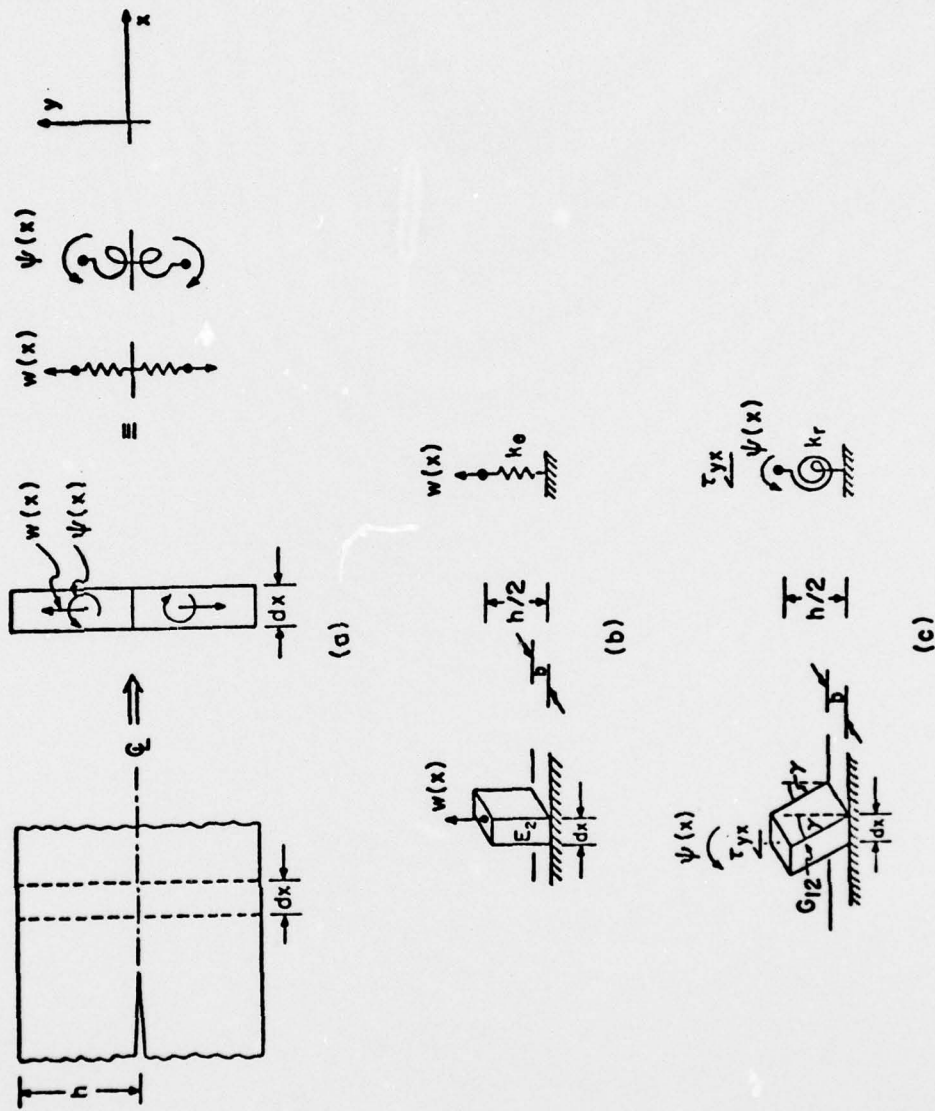
Fig. 3   Models for calculating the foundation parameters of the orthotropic double cantilever beam.

SECTION 4

NUMERICAL STABILITY AND CONVERGENCE CRITERIA

FOR EQUATIONS FOR DYNAMIC FRACTURE IN

DCB COMPOSITE SPECIMENS

ABSTRACT

The stability and convergence criteria for numerical solutions
of the governing equations for dynamic crack propagation in DCB uni-
directional composite specimens are determined. The stability criteria
are given explicitly and it is concluded that the convergence require-
ments will be met automatically by solutions which satisfy the stability
criteria.

INTRODUCTION

The governing differential equations for dynamic crack propagation in double cantilever beam (DCB) specimens generally require a numerical solution. These equations are frequently restated in their finite-difference approximations as in the cases for the homogeneous isotropic DCB [1] and for the homogeneous orthotropic DCB [2]. The numerical evaluation of the finite-difference equations requires the selection of temporal and spatial interval sizes.

Heuristic suitable interval sizes for the finite-difference isotropic DCB equations have been obtained by trial-and-error [1]. However, no analytical verification of suitable interval sizes has been obtained for this problem. Furthermore, suitable interval sizes for the orthotropic DCB have not been obtained either by trial-and-error or analytically. The purpose of this report is to present an analytical derivation of suitable interval sizes for the solution of the finite-difference orthotropic DCB equations for Mode I dynamic crack propagation. The analogous suitable interval sizes for the isotropic DCB are contained within these results.

If Ξ_i represent the exact solutions of the partial differential equations and Ξ_j' represent the exact solutions of the finite-difference equations and Ξ_k'' represent the numerical solutions of the finite-difference equations, then determining the conditions under which $\left(\Xi_j' \to \Xi_i\right)_{i=j=1,2,\ldots,N}$ is the problem of convergence and determining the conditions under which $\left(\Xi_j' \to \Xi_k''\right)_{j=k=1,2,\ldots,\ N}$ is small throughout the region of integration is the problem of stability, where N is the number of differential equations. In the analyses which follow, the problem of stability will be emphasized

-93-

as it will be shown that for the homogeneous orthotropic DCB equations, solution stability will ensure solution convergence.

THEORETICAL ANALYSIS

Governing Equations

The governing differential equations for Mode I dynamic crack propagation in orthotropic DCB specimens are [2]

$$\frac{\partial^2 Y}{\partial \zeta^2} + \frac{10G_{12}}{E_1}\left(\frac{\partial W}{\partial \zeta} - Y\right) - \langle\theta_c-\theta\rangle^\circ \frac{5G_{12}}{E_1} Y = \frac{1}{12}\frac{\partial^2 Y}{\partial \tau^2} \tag{1}$$

and

$$\frac{\partial^2 W}{\partial \zeta^2} - \frac{\partial Y}{\partial \zeta} - \langle\theta_c-\theta\rangle^\circ \frac{12E_2}{5G_{12}} W = \frac{E_1}{10G_{12}}\frac{\partial^2 W}{\partial \tau^2}. \tag{2}$$

These equations are written in terms of the following nondimensional variables:

Independent – $\zeta = \dfrac{x}{h}$ and $\tau = \left(\dfrac{E_1}{12\rho}\right)^{1/2}\dfrac{t}{h}$

Dependent – $W = w\left(\dfrac{K_e}{\theta_c}\right)^{1/2}$ and $Y = \psi h\left(\dfrac{K_e}{\theta_c}\right)^{1/2}$

where

x = longitudinal coordinate along the beam (crack propagation direction)

t = time

w = transverse displacement of beam on elastic foundation

ψ = rotation of beam on elastic foundation

h = half-height of DCB

b = width of DCB

ρ = mass density of the DCB

E_1 = extensional modulus in x-direction

E_2 = extensional modulus transverse to x-direction

G_{12} = 1-2 plane shear modulus

$K_e = \dfrac{2E_2 b}{h}$

$K_r = \dfrac{\kappa G_{12} bh}{2}$

κ = shear coefficient

θ = $K_e w^2 + K_r \psi^2$

θ_c = $2b\gamma_d$

γ_d = dynamic surface fracture energy

$<\ >^\circ$ = singularity function which is one (1) for positive

argument and zero (0) otherwise.

The respective finite-difference formulations of eqns. (1) and (2) are

$$\frac{1}{(\Delta\zeta)^2}\left\{Y(\zeta+\Delta\zeta,\ \tau) - 2Y(\zeta,\tau) + Y(\zeta-\Delta\zeta,\ \tau)\right\}$$

$$+ \frac{5G_{12}}{E_1(\Delta\zeta)}\left\{W(\zeta+\Delta\zeta,\ \tau) - W(\zeta-\Delta\zeta,\ \tau)\right\} - \frac{5G_{12}}{E_1}\left[2 + <\theta_c-\theta>^\circ\right]Y(\zeta,\tau)$$

$$= \frac{1}{12(\Delta\tau)^2}\left\{Y(\zeta,\ \tau+\Delta\tau) - 2Y(\zeta,\tau) + Y(\zeta,\ \tau-\Delta\tau)\right\}. \qquad (3)$$

-96-

and

$$\frac{1}{(\Delta\zeta)^2}\left\{W(\zeta+\Delta\zeta,\ \tau)\ -\ 2W(\zeta,\tau)\ +\ W(\zeta-\Delta\zeta,\ \tau)\right\}$$

$$-\ \frac{1}{2\Delta\zeta}\left\{Y(\zeta+\Delta\zeta,\ \tau)\ -\ Y(\zeta-\Delta\zeta,\ \tau)\right\}\ -\ <\theta_c-\theta>^\circ\ \frac{12E_2}{5G_{12}}\ W(\zeta,\tau)$$

$$=\ \frac{E_1}{10G_{12}(\Delta\tau)^2}\left\{W(\zeta,\ \tau+\Delta\tau)\ -\ 2W(\zeta,\tau)\ +\ W(\zeta,\ \tau-\Delta\tau)\right\} \qquad (4)$$

where Δ is the incremental finite-difference operator.

Error Equations

It is useful to define the following variables:

$$Y_{j,k}\ \equiv\ Y(\zeta,\tau)\ ;\qquad Y_{j\pm 1,k\pm 1}\ \equiv\ Y(\zeta\pm\Delta\zeta,\ \tau\pm\Delta\tau)$$

$$\tag{5}$$

$$W_{j,k}\ \equiv\ W(\zeta,\tau)\ ;\qquad W_{j\pm 1,k\pm 1}\ \equiv\ W(\zeta\pm\Delta\zeta,\ \tau\pm\Delta\tau)$$

where j and k are integers. If $Y_{j,k}$ and $W_{j,k}$ represent the exact solution of the finite-difference equations (3) and (4), then the numerical solution of the finite-difference equations may be written as

$$(Y+\lambda)_{j,k}\quad \text{and}\quad (W+\mu)_{j,k} \qquad (6)$$

where λ and μ are numerical errors associated with Y and W, respectively.

Substitution of eqns. (5) into eqns. (3) and (4) gives

-97-

$$\frac{Y_{j+1,k} - 2Y_{j,k} + Y_{j-1,k}}{(\Delta\zeta)^2} + A\frac{W_{j+1,k} - W_{j,k}}{\Delta\zeta} - (A+B)Y_{j,k}$$

$$= D\frac{Y_{j,k+1} - 2Y_{j,k} + Y_{j,k+1}}{(\Delta\tau)^2} \tag{7}$$

and

$$A\frac{W_{j+1,k} - 2W_{j,k} + W_{j-1,k}}{(\Delta\zeta)^2} - A\frac{Y_{j+1,k} - Y_{j,k}}{\Delta\zeta} - CW_{j,k}$$

$$= \frac{W_{j,k+1} - 2W_{j,k} + W_{j,k-1}}{(\Delta\tau)^2} \tag{8}$$

where

$$A \equiv \frac{10G_{12}}{E_1} \qquad ; \qquad B \equiv \langle\theta_c - \theta\rangle^\circ\,\frac{5G_{12}}{E_1}$$

$$C \equiv \langle\theta_c - \theta\rangle^\circ\,\frac{24E_2}{E_1} \quad ; \qquad D \equiv \frac{1}{12}\,.$$

Similarly, substitution of eqns. (6) into eqns. (3) and (4) gives

$$\frac{(Y+\lambda)_{j+1,k} - 2(Y+\lambda)_{j,k} + (Y+\lambda)_{j-1,k}}{(\Delta\zeta)^2} + A\frac{(W+\mu)_{j+1,k} - (W+\mu)_{j,k}}{(\Delta\zeta)^2} - \cdots \tag{9}$$

and

$$A\frac{(W+\mu)_{j+1,k} - 2(W+\mu)_{j,k} + (W+\mu)_{j-1,k}}{(\Delta\zeta)^2} - \cdots \tag{10}$$

-98-

Substracting eqn. (7) from eqn. (9) and eqn. (8) from eqn. (10) gives

$$\frac{\lambda_{j+1,k} - 2\lambda_{j,k} + \lambda_{j-1,k}}{(\Delta\zeta)^2} + A\frac{\mu_{j+1,k} - \mu_{j,k}}{\Delta\zeta} - (A+B)\lambda_{j,k}$$

$$= D\frac{\lambda_{j,k+1} - 2\lambda_{j,k} + \lambda_{j,k+1}}{(\Delta\tau)^2} \qquad (11)$$

and

$$A\frac{\mu_{j+1,k} - 2\mu_{j,k} + \mu_{j-1,k}}{(\Delta\zeta)^2} - A\frac{\lambda_{j+1,k} - \lambda_{j,k}}{\Delta\zeta} - C\mu_{j,k}$$

$$= \frac{\mu_{j,k+1} - 2\mu_{j,k} + \mu_{j,k-1}}{(\Delta\tau)^2} \qquad . \qquad (12)$$

It can be seen that the errors λ and μ must satisfy the same equations as their respective associated nondimensional variables Y and W. This is a consequence of the linearity of the governing partial differential equations (1) and (2).

Solution Stability

The solution stability analysis which follows is generally attri-
buted to J. von Neumann although the first detailed discussion was pre-
sented by O'Brien, Hyman and Kaplan [3]. The procedure is to form Fourier
expansions of lines of errors and to follow the progress of the general
terms of the expansions. For the problem under consideration, these Fourier
expansions may be written as

-99-

$$\lambda(\zeta) = \sum_n \delta_n e^{i\beta_n \zeta} \quad \text{and} \quad \mu(\zeta) = \sum_n \varepsilon_n e^{i\beta_n \zeta}. \tag{13}$$

At each line of computation, groups of errors are introduced which propagate forward in accordance with eqns. (11) and (12).

Because of superposition, it is necessary to consider only the single error term $e^{i\beta\zeta}$ where β is any member of the $\{\beta_n\}$, each of which is any real number. So, solutions of eqns. (11) and (12) which reduce to $e^{i\beta\zeta}$ when $\tau=0$ are sought. In accordance with [3], let

$$\begin{Bmatrix} \lambda \\ \mu \end{Bmatrix}_{j,k} = \begin{Bmatrix} \delta \\ \varepsilon \end{Bmatrix} e^{\alpha\tau} e^{i\beta\zeta} \tag{14}$$

where $\alpha = \alpha(\beta)$ is generally complex. In order that the original error $e^{i\beta\zeta}$ shall not grow as τ increases, it is necessary and sufficient that $\left| e^{\alpha\Delta\tau} \right| \le 1$, [3].

Substitution of eqn. (14) into eqn. (11) and eqn. (14) into eqn. (12) gives, respectively,

$$\begin{bmatrix} 2(\cos\beta\Delta\zeta-1)r^2 - D(\eta-2+\frac{1}{\eta}) - (A+B)\Delta\tau^2 & A(e^{i\beta\Delta\zeta}-1)r\Delta\tau \\ \\ -A(e^{i\beta\Delta\zeta}-1)r\Delta\tau & 2A(\cos\beta\Delta\zeta-1)r^2 \\ & -(\eta-2+\frac{1}{\eta}) - C\Delta\tau^2 \end{bmatrix} \begin{Bmatrix} \delta \\ \\ \varepsilon \end{Bmatrix} \begin{Bmatrix} 0 \\ \\ 0 \end{Bmatrix} \tag{15}$$

where $\eta \equiv e^{\alpha\Delta\tau}$ and $r \equiv \dfrac{\Delta\tau}{\Delta\zeta}$. A non-trivial solution requires that the determinant of the coefficient matrix be zero. Thus,

-100-

$$[\Phi \cdot \Psi] + [A^2(e^{i\beta\Delta\zeta} - 1)r^2 - (A+B)\Psi - C\Phi]\Delta\tau^2 + [(A+B)C]\Delta\tau^4 = 0 \qquad (16)$$

where $\qquad \Phi = 2(\cos\beta\Delta\zeta - 1)r^2 - D(\eta - 2 + \frac{1}{\eta})$

and $\qquad \Psi = 2A(\cos\beta\Delta\zeta - 1)r^2 - (\eta - 2 + \frac{1}{\eta})$.

Because the coefficients of $\Delta\tau^n$ are of the same order and by invoking the requirement that $\Delta\tau \ll 1$, it can be seen that the first-order approximation to the solution of eqn. (16) is satisfied by requiring that the coefficient of $\Delta\tau^\circ$ is approximately zero. Thus, $\Phi \cdot \Psi = 0$ gives

$$\Lambda^2 - 2(\cos\beta\Delta\zeta - 1)(A + \frac{1}{D})r^2\Lambda + \frac{4A}{D}(\cos\beta\Delta\zeta - 1)^2 r^4 = 0 \qquad (17)$$

where $\Lambda \equiv \eta - 2 + \frac{1}{\eta}$. The solution of eqn. (17) may be obtained by use of the quadratic equation as

$$\Lambda = (\cos\beta\Delta\zeta - 1)r^2 \left[(A + \frac{1}{D}) \pm \sqrt{\left(A + \frac{1}{D}\right)^2 - \frac{4A}{D}}\right]. \qquad (18)$$

Noting that $\left(A + \frac{1}{D}\right)^2 - \frac{4A}{D} = \left(A - \frac{1}{D}\right)^2$, eqn. (18) gives

$$\begin{Bmatrix} \Lambda_1 \\ \Lambda_2 \end{Bmatrix} = \begin{Bmatrix} A \\ \frac{1}{D} \end{Bmatrix} 2(\cos\beta\Delta\zeta - 1)r^2 . \qquad (19)$$

Note that because $A \equiv \frac{10G_{12}}{E_1}$ and $D \equiv \frac{1}{12}$ are always real and positive and because $-1 \leq \cos\beta\Delta\zeta \leq 1$, the maximum value of both Λ_1 and Λ_2 is

zero. Also, the minimum values of Λ_1 and Λ_2 occur when $\cos\beta\Delta\zeta = -1$.

From the definition of Λ,

$$\Lambda_{1,2} = \eta_{1,2} - 2 + \frac{1}{\eta_{1,2}}$$

or,

$$\eta_{1,2}^2 - (2 + \Lambda_{1,2})\eta_{1,2} + 1 = 0 , \qquad (20)$$

which has the solutions

$$\eta_{1,2} = \gamma_{1,2} \pm \sqrt{\gamma_{1,2}^2 - 1} \qquad (21)$$

where $\gamma_{1,2} \equiv 1 + \dfrac{\Lambda_{1,2}}{2}$. Recall that the necessary and sufficient conditions on η are that $\left| e^{\alpha\Delta\tau} \right| = \left| \eta_{1,2} \right| \leq 1$. It can be shown, that these necessary and sufficient conditions are satisfied if $\left| \gamma_{1,2} \right| \leq 1$. Note that if $\left| \gamma_{1,2} \right| \leq 1$, $\sqrt{\gamma_{1,2}^2 - 1} = \sqrt{-1}\sqrt{1-\gamma_{1,2}^2} = i\sqrt{1-\gamma_{1,2}^2}$ where $i \equiv \sqrt{-1}$. Thus, from eqn. (21) it can be seen that $\eta_{1,2}$ are complex numbers with a modulus of one (1). Further, the requirements on $\gamma_{1,2}$ may be written as

$$-1 \leq 1 + \frac{\Lambda_{1,2}}{2} \leq 1 \qquad (22)$$

where the definition of $\gamma_{1,2}$ has been used. Recall that the maximum value of $\Lambda_{1,2}$ is zero; thus, the right-hand inequality has been satisfied already. The left-hand inequality imposes the other limit on $\Lambda_{1,2}$, namely

$$\Lambda_{1,2} \geq -4 . \qquad (23)$$

Finally, by noting that the minimum values of $\Lambda_{1,2}$ are obtained when $\cos\beta\Delta\zeta = -1$, eqns. (19) and (23) may be combined to give the simultaneous requirements

$$2A \ (-2)(r^2) \geq -4$$

$$2 \frac{1}{D} \ (-2)(r^2) \geq -4$$

or

$$r^2 \leq \frac{1}{A}$$

(24)

$$r^2 \leq D \ .$$

By inserting the definitions for r, A and D into eqns. (24), the integration interval size requirements become

$$\frac{\Delta\tau}{\Delta\zeta} \leq \sqrt{\frac{E_1}{10G_{12}}}$$

(25)

$$\frac{\Delta\tau}{\Delta\zeta} \leq \sqrt{\frac{1}{12}}$$

where the appropriate $\frac{\Delta\tau}{\Delta\zeta}$ is the smaller of the two. Thus, eqns. (25) represent the criteria to ensure solution stability. Furthermore, eqns. (25) require that independent of the material constitutive parameters E_1 and G_{12}, r should always be less than $\sqrt{1/12}$. Therefore, eqns. (25) contain within them the solution convergence criteria also because $r \leq 1$ is the necessary and sufficient condition for solution convergence [3,4].

REFERENCES

1. G.T. Hahn et al., "Fast Fracture Resistance and Crack Arrest in Structural Steels", SSC-242 Progress Report, 1973.

2. "Governing Equations for Mode I Dynamic Fracture in Orthotropic DCB Specimens with External Dynamic Interactions", Section 3 of this Report.

3. G.G. O'Brien, M.A. Hyman and S. Kaplan, "A Study of the Numerical Solution of Partial Differential Equations", Journal of Mathematical Physics, Vol. 29, 1951, pp. 223-251.

4. R. Courant, K. Friedrichs and H. Lewy, "Uber die Partiellen Differenzengleichungen der Mathematischen Physik", Math. Ann., Vol. 100, 1928, pp. 32-74.

REFERENCES

1. C.F. Naim et al., "Fast Fracture Resistance and Crack Arrest in Structural Steels", SSC-242 Technical Report, 1973.

2. "Governing Equations for Mode I Dynamic Fracture in Unsymmetric DCB Specimens with External Dynamic Interactions", Section 2 of this Report.

3. G.G. O'Brien, M.A. Hyman and S. Kaplan, "A Study of the Numerical Solution of Partial Differential Equations", Journal of Mathematical Physics, Vol. 29, 1951, pp. 223-251.

4. R. Courant, K. Friedrichs and H. Lewy, "Über die Partiellen Differenzengleichungen der Mathematischen Physik", Math. Ann., Vol. 100, 1928, pp. 32-74.

SECTION 5

CONDUCTIVE GRID VELOCITY MEASUREMENT SYSTEM

ABSTRACT

A conductive grid system which is capable of measuring the crack-tip velocity profile has been designed, built and proof-tested.

VELOCITY MEASUREMENT SYSTEM

A conductive grid velocity measurement system has been designed, built and proof-tested. This system which is capable of providing the crack-tip velocity profile (crack-tip velocity as a function of crack length) is shown in Fig. 1. Lines of brittle conductive silver paint are painted perpendicular to the anticipated crack path. The silver paint grid forms part of an electrical circuit whose elements are sequentially interrupted as the crack advances and fractures the brittle paint lines. The crack velocity can be calculated from knowledge of the location of the conductive lines and the time at which each line fractures.

The design of the circuit and the choice of the resistors are such that the output DC voltage decreases by an equal amount each time the fracture of a silver paint conductive line occurs. Because the graphite epoxy specimens are conductive, a thin insulating coating of epoxy is applied to the specimen surface prior to the application of the silver paint grid. Preliminary tests have shown that the fracture strains of the silver paint and the epoxy matrix are essentially the same.

A modified video tape recorder is used to record the output of the circuit. The use of the tape recorder eliminates any trigger requirements in capturing the dynamic circuit output during fracture propagation. The recorder can be started well in advance of the rapid fracture event and run throughout the loading of the specimen. The video tape recorder has a gated playback capability which allows the selection of any portion of the tape to be played in the "still" mode. The tape recorder output is displayed in the "still" mode on an

oscilloscope where time intervals between successive grid line fractures can be measured.

Unidirectional 90° (fibers perpendicular to the loading axis) Hercules AS/3501 graphite epoxy panels, 35.56 cm wide x 15.24 cm high x 0.127 cm thick (14 in x 6 in x 0.05 in) with a 5.08 cm (2 in) Mode I edge notch have been tested. By varying the loading conditions in the tensile test, crack velocities from 30.48 m/sec (100 ft/sec) to 2743 m/sec (9000 ft/sec) have been measured.
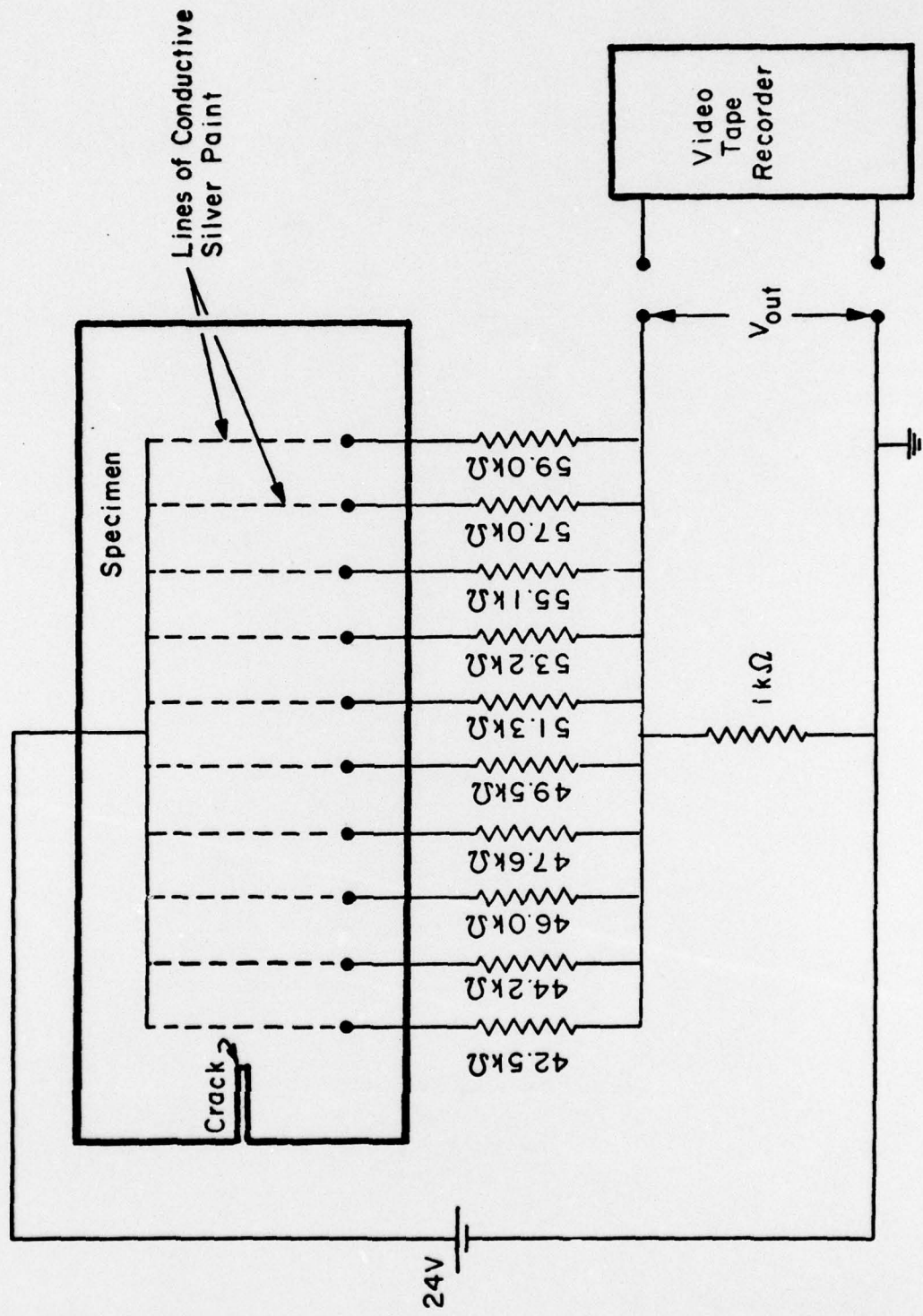
Fig. 1 Experimental circuit for crack velocity measurement using the conductive grid.

SECTION 6

CONCLUSIONS AND RECOMMENDATIONS

The results obtained so far have been described in Sections 1 through 5 of this report and are summarized in the abstracts of the respective sections. Therefore, these results will not be repeated here except for the brief comments in the next paragraph.

In formulating a total framework for dynamic fracture, three major categories of the problem may be defined. These are

        1.   Intralaminar-interfiber fracture,

        2.   Intralaminar-transfiber fracture, and

        3.   Interlaminar fracture.

Note that Section 2 dealt with the theoretical dynamic crack extension force for intralaminar-transfiber fracture. Sections 3 and 4 dealt with the analytical aspects of both the intralaminar-interfiber and the intra-laminar-transfiber fracture problems. Section 5 described an experimental system which is capable of measuring crack-tip velocity profiles in the determination of experimental dynamic fracture toughness.

The ultimate goals of this research are (1) to establish firm theoretical and experimental bases for dynamic fracture and crack arrest in fiber composites, and (2) to devise standardization techniques and procedures for the measurement of dynamic toughness and crack arrest capability of advanced fiber composites. At this point, there remains a considerable number of specific aspects of dynamic fracture and crack

-113-

arrest in composites which require both experimental and theoretical analysis. A detailed delineation of the various research requirements to achieve these goals is beyond the scope of this program. Therefore, a limited list of specific recommendations are offered:

1. Experimentally measure the dynamic fracture toughness of Hercules AS/3501 graphite epoxy composites for intra-laminar-interfiber fracture.

2. Conduct numerical analysis for the orthotropic DCB indicated in Sections 3 and 4 of this report.

3. Derive a dynamic crack extension force via the velocity correction factor procedure for intralaminar-interfiber fracture.

4. Establish the required correlations to bring the three (3) previous recommendations into consistency.

These four (4) recommendations provide a meaningful framework for the intralaminar-interfiber dynamic fracture problem which based upon this report can be conducted in a straightforward manner.

QUANTITY

Naval Air Systems Command
Washington, D.C.
ATTN: AIR-954
  For distribution as follows:
    AIR-52032D
    AIR-954

9

3
6

Office of Naval Research (Code 472)
Washington, D.C. 20350

1

Office of Naval Research, Boston
495 Summer Street
Boston, MA 02210
ATTN: Dr. L.H. Peebles

1

Naval Research Laboratory
(Code 6306 and 6120)
Washington, D.C. 20350

2

Naval Ordnance Laboratory
Code 234
White Oak, Silver Spring, MD 20910

Air Force Materials Laboratory
Wright-Patterson Air Force Base, OH 45433
ATTN: LC 1
     LN 1
     LTF 1
     LAE 1

4

Air Force Flight Dynamics Laboratory
Wright-Patterson Air Force Base, OH 45433
ATTN: FDTC

1

Defense Ceramic Information Center
Battelle Memorial Institute
505 King Avenue
Columbus, OH 43201

1

Illinois Institute of Technology Research Institute
10 West 35th Street
Chicago, IL 60616
ATTN: Dr. R. Cornish

1

Brunswick Corporation
Technical Products Division
325 Brunswick Lane
Marion, VA 24354

1

(continued)

Director   1
Plastics Technical Evaluation Center
Picatinny Arsenal
Dover, NJ 07801

The Rand Corporation   1
1700 Main Street
Santa Monica, CA   90406

HITCO   1
1600 W. 135th St.
Gardena, CA 90406

AVCO Corporation   1
Applied Technology Division
Lowell, MA 01851

Department of the Army   1
Army Materials & Mechanics Research Center
Watertown, MA 02172

North American Aviation   1
Columbus Division
4300 E. Fifth Avenue
Columbus, OH 43216

Rockwell International Corp   1
12214 Lakewood Blvd
Downey, CA 90241
ATTN: Mr. C.R. Rousseau

McDonnell-Douglas Corporation   1
Douglas Aircraft Company
3855 Lakewood Blvd
Long Beach, CA 90801
ATTN: Mr. R.J. Palmer

General Electric Company   1
Valley Forge Space Center
Philadelphia, PA 19101

Monsanto Research Corporation   1
1515 Nicholas Road
Dayton, OH 45407

Material Sciences Corporation   1
1777 Walton Road
Blue Bell, PA 19422

(continued)

U.S. Army Air Mobility R&D Laboratory   1
Fort Eustis, VA
ATTN: SAVDL-EU-SS (Mr. J. Robinson)

B.F. Goodrich Aerospace & Defense Products   1
500 South Main Street
Akron, OH 44318

Great Lakes Research Corporation   1
P.O. Box 1031
Elizabethton, TN

Lockheed California Co.   1
Box 551
Burbank, CA 91520
ATTN: Mr. J.H. Wooley

Lockheed Missiles & Space Co.   1
Sunnyvale, CA 94088
ATTN: Mr. H.H. Armstrong, Dept. 62-60

TRW Inc.   1
23555 Euclid Ave
Cleveland, OH 44117

E.I. DuPont de Nemours & Co.   1
Textile Fibers Dept
Wilmington, DE 19898
ATTN: Dr. C. Zweben

Bell Aerospace Co.   1
Buffalo, NY 14240
ATTN: Mr. F.M. Anthony

Union Carbide Corporation   1
Chemicals and Plastics
One River Road
Bound Brook, NJ 08805

General Dynamics   1
Convair Aerospace Division
P.O. Box 748
Ft. Worth, TX 76101
ATTN: Tech Library

General Dynamics   1
Convair Division
P.O. Box 1128
San Diego, CA 92138
ATTN: Mr. W. Scheck; Dept 572-10

QUANTITY

TRW Inc,
Systems Group
One Space Park
Bldg. 01; Rm 2171
Redondo Beach, CA 90278

McDonnell Douglas Corp
McDonnell Aircraft Co.
P.O. Box 516
St. Louis, MO 63166
ATTN: Mr. R. Jurgens

Fiber Materials Inc
Biddeford Industrial Park
Biddeford, ME 04005
ATTN: Mr. J. Herrick

General Electric
R&D Center
Box 8
Schnectady, NY 12301
ATTN: Mr. W. Hillig

Stanford Research Institute
333 Ravenswood Ave.
Bldg. 102B
Menlo Park, CA 94025
ATTN: Mr. M. Maximovich

North American Aviation
Columbus Division
4300 E. Fifth Avenue
Columbus, OH 43216

University of California
Lawrence Livermore Laboratory
P.O. Box 808
Livermore, CA 94550
ATTN: Mr. T.T. Chiao

Hercules Incorporated
Magna, UT 84044
ATTN: Mr. E.G. Crossland

Northrop Corporation
3901 W. Broadway
Hawthorne, CA 90250
ATTN: Mr. R.L. Jones; Dept 3870-62

(continued)

-119-

Naval Air Propulsion Test Center
Trenton, NJ 08628
ATTN: Mr. J. Glatz   1

Naval Ship R&D Center
Annapolis, Marryland 21402
ATTN: Mr. M. Silvergleit (Code 2823)

Commander
U.S. Naval Weapons Center
China Lake, CA 92555

Celanese Research Company
Box 1000
Summit, NJ 07901
ATTN: Mr. R.J. Leal

Naval Ship Engineering Center
Code 6101E
Navy Department
Washington, D.C. 20360

Naval Sea Systems Command
Code SEA-035
Washington, D.C. 20360

NASA Headquarters
Code RV-2 (Mr. N. Mayer)
600 Independence Ave., S.W.
Washington, D.C. 20546

The Boeing Company
Aerospace Division
P.O. Box 3707
Seattle, WA 98124

Boeing-Vertol Co.
P.O. Box 16858
Philadelphia, PA 19142
ATTN: Dept. 1951

Commander
Naval Air Development Center
Warminster, PA 18974   3
ATTN: Aero Materials Dept.
      Aero Structures Dept.
      Radomes Section

(continued)

Naval Ship Research & Development Center   1
Washington, D.C.
ATTN: Mr. M. Krenzke, Code 727

NASA   1
Lewis Research Center
21000 Brookpark Road
Cleveland, OH 44135

NASA
Langley Research Center
Hampton, VA 23368

United Aircraft Corporation   1
United Aircraft Research Laboratories
E. Hartford, CT 06108

United Aircraft Corporation   1
Pratt & Whitney Aircraft Division
East Hartford, CT 06108

United Aircraft Corporation   1
Hamilton-Standard Division
Windsor Locks, CT 06096
ATTN: Mr. T. Zajac

United Aircraft Corporation
Sikorsky Aircraft Division
Stratford, CT 06602
ATTN: Mr. J. Ray

Union Carbide Corporation   1
Carbon Products Division
P.O. Box 6116
Cleveland, OH 44101

Philco-Ford Corporation   1
Aeronutronic Division
Ford Road
Newport Beach, CA 92663

Grumman Aerospace Corporation   1
Bethpage, L.I., New York 11714
ATTN: Mr. G. Lubin, Plant #12